Simple, economical methods for electrical access to nanostructures used for characterizing and welding individual silver nanowires

by

Arash Vafaei

A thesis
presented to the University of Waterloo
in fulfillment of the
thesis requirement for the degree of
Master of Applied Science
in
Electrical and Computer Engineering - Nanotechnology

Waterloo, Ontario, Canada, 2013

I hereby declare that I am the sole author of this thesis. This is a true copy of the thesis, including any required final revisions, as accepted by my examiners.

I understand that my thesis may be made electronically available to the public.

Abstract

Elongated nanostructures have attracted a great deal of interest due to unique optical, electrical and physical properties. In particular, silver nanowires and nanobeams have proven to be top contenders for a variety of applications. Due to their nano-sized dimensions, however, electrical access to individual nanowires is difficult and expensive. Here, a simple and economical procedure was designed to electrically contact small elongated structures using common facilities available at most universities. A common lithographic procedure is used to pattern gold pads and electrodes on top of nanowires already dispersed on a substrate.

This process is tested by first characterizing, using a 4-point-probe measurement, a novel nanobeam created by fusing silver nanodisks. The resistivity of the nanobeams was found to be as low as $2.7\text{x}10^{-8}$ Ω·m, which is only slightly above that of bulk silver. These measurements corroborate modeling done by another group that the nanodisks align to create a nearly continuous crystal rather than disjointed grains.

In the second application, Joule-heating was used to actualize a reliable weld between silver nanowires synthesized using the polyol method. The nanowires were situated in series between two metal pads, and a procedure was designed to use electrical current to break down intermediate layers without destroying the nanowires themselves.

In the last enterprise, individual silver nanowires were isolated between two gold pads and then using the same electrical recipe used for welding nanowires, the contact resistance was reduced to a negligible portion of its original value. It was found that due to the reduction in contact resistance, the 2-point-probe resistivity of the nanowire was similar to those conducted using 4 probes. The invented procedure can thus allow accurate resistivity measurements of individual metal nanowires to be done with only 2 contacts rather than 4, thereby simplifying contact fabrication and allowing appropriate contacts to be deposited on nanowires as short as 4 μm using standard photolithography.

Acknowledgements

I would like to first thank Irene Goldthorpe for the excellent job she did as my supervisor. The growth and character of an intellectual comes from mature independence and Irene has fostered that trait unlike any other role model. Also thanks for being my editor, this thesis would not have been possible without your dedication.

I would like to thank Richard Barber, Nathan Nelson-Fitzpatrick, Brian Goddard, and Rodello Salandanan for doing everything in their power to make sure my little project goes on. I could not have done it without your help.

I would also like to thank Anming Hu, for timely advice, a great collaboration, and an unflinching dedication.

Dedication

I would like to dedicate this thesis to my mother and father, for making sure I'm alive long enough get here. :-)

I would also like to dedicate this thesis to VDH. It's not every day a lost young man has his mind opened to a whole new world that existed unbeknownst to him,

Table of Contents

List of Figures

Chapter 1

Introduction

1.1 Nanowires

1.1.1 In general

Nanowires and nanobeams are objects with two nanosized dimensions and one elongated dimension of several microns or more. As a class of nanostructures, nanowires contain a great deal of variety and applicability. For the purposes of this thesis, elongated structures with rectangular cross-sections (studied in Chapter 3) will be called nanobeams and structures with pentagonal cross-sections (studied in Chapters 4 and 5) will be called nanowires. For the purposes of this introduction however they will both be referred to as nanowires.

Due to the unique shape and physical properties of nanowires they have found uses in many segments of engineering. Applications in the fields of optics [1, 2, 3], electrical devices [3, 4], chemistry [5] and many more have been proposed. These structures have been incorporated into solar cells [6], sensors [5, 7, 8, 9], and integrated circuits [10].

Silver nanowires in particular are of interest due to the fact that silver has the highest heat and electrical conductivity of any metal. Silver nanowires have been used for applications such as plasmonic waveguides [11], water antibacterial treatment [12], and sensing [13]. There are several methods of creating nanowires and they can be generally summarized as top-down and bottom-up. The top-down approach often involves the deposition of the nanowire material on the substrate and requires patterning to create the desired nanowire shape. The bottom-up method however uses the constituents of the nanowires, often in self-assembly, to build devices larger than the constituents, without patterning. The nanowires studied in this thesis are synthesized using such bottom-up approaches.

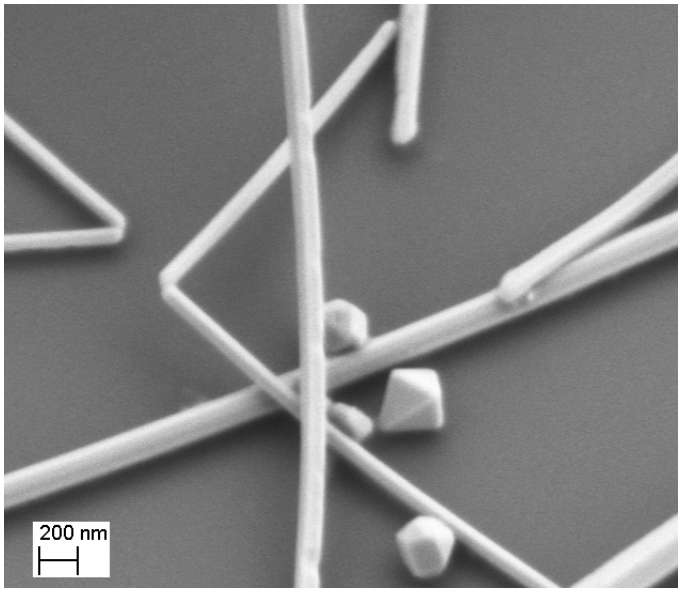

Figure 1.1: An SEM picture of nanowires with pentagonal cross-sections synthesized by the polyol method. (Reproduced with permission from Anming Hu)

In this project a simple, accessible, and economical method for accessing nanowires electrically is desired, and so a procedure is invented to characterize, probe, and weld novel nanowires. The two nanowires used in this project are polyol self-assembled nanobeams, and polyol synthesized pentagonally-twinned nanowires.

1.1.2 Polyol synthesis

One of the more popular methods of creating silver nanostructures with smooth surfaces and good crystallinity is the polyol process. This process can create a large number of nanostructures relatively cheaply and quickly. The polyol process in the simplest sense is the heating of a polyol (alcohol with multiple hydroxyl groups) and a metal salt precursor mixed together to produce metal precipitates, while a capping polymer restricts growth in certain crystal directions creating distinct shapes [14].

In this project, nanowires created by the process described in [15], which is a modification of the standard method common in literature [16], was used. In this procedure polyvinylpyrrolidone (PVP) ((C6H9NO)n, K25, M.W.= 24000, Alfa Aesar) and 12.5 mg silver chloride (AgCl, Alfa Aesar) were mixed with 40 ml ethylene glycol (EG, Fisher Chemical) inside a round-bottom flask. Ethylene glycol served as the polyol while AgCl

served as the precursor and PVP as the polymer capping agent. The mixture was heated to 160-170^{o}C for 30 minutes to create the seed particles required for the creation of the wires. 10 ml of solution of 110 mg of silver nitrate in ethylene glycol heated to the same temperature was then added into the mixture stirring vigorously for 4 hours. At this stage the PVP in the solution attaches itself to the sides of the already elongated structures, passivating the surfaces to reaction. With the sides refusing to accept more silver ions and the ends remaining reactive, a rapid growth in the axial direction occurs resulting in the pentagonally-twinned nanowires shown in Figure 1.1. A twinned structure consists of single crystalline parts joined together at a twin grain boundary. The polyol nanowires have five crystal grains, resulting in a pentagonal cross-section with 5 {100} surface facets. The grain boundaries in this case run down the longitudinal axis. Figure 1.2 shows a diagram of the nanowires clearly showing the grain boundaries.

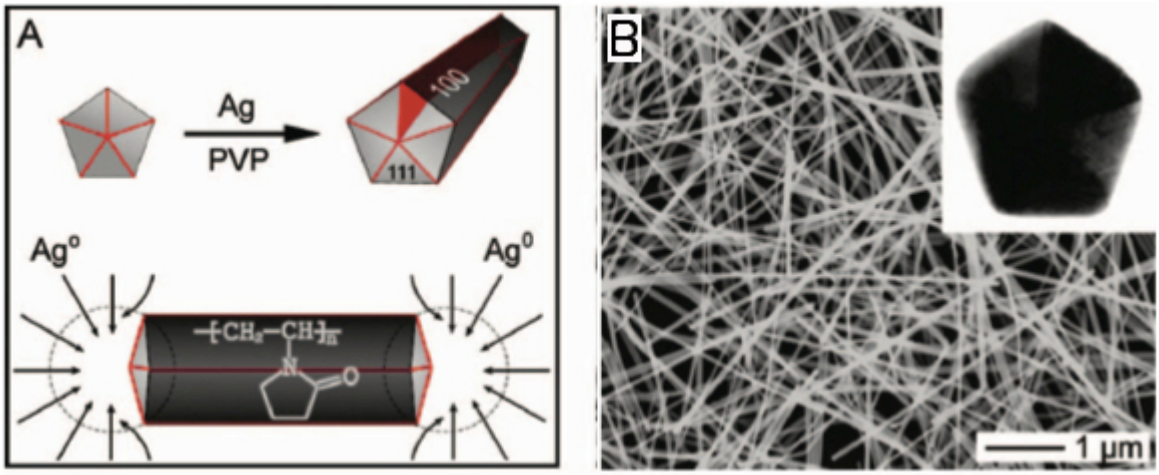

Figure 1.2: A diagram of the pentagonally-twinned structure of silver nanowires is shown in A, while B shows the real polyol synthesized nanowires and the pentagonal face. Reprinted with permission from [17]

These nanowires will be used in Chapter 4 to demonstrate electrically induced Joule-heat welding of two metallic nanostructures in near vicinity. Although Joule-heat welding of nanowires has been done before [18, 19], it has never been done with this type of nanowire or with the economical in-air methodology invented.

The same type of nanowire is used in Chapter 5 although with a slightly different polyol procedure, purchased from Blue Nano Inc. Joule heating is used to reduce contact resistance to be much lower than the resistance of the nanowire itself. This has great appli-

cations in various 2-point-probe experiments, where contact resistance cannot be ignored yet the projects demand it.

1.1.3 Synthesis through self-assembly

In Chapter 3 of this thesis the electrical properties of silver nanobeams constructed using room temperature joining of hexagonal and triangular nanodisks are investigated. The nanodisks are created as per [20], using the polyol method (see Section 1.1.2). The disks exist in solution with a variety of sizes ranging from 30-300 nm for the longest dimension [21]. A twin plane is located parallel to the main surface of the disks in-between the two faces. The disks are then joined using the atomic attraction of silver atoms with PMMA as a capping agent for site specific joining. In particular the PMMA attaches to the faces of the plates where surface energy is the highest and thus allows joining only at the edges. Figure 1.3 illustrates the disks used and the final product.

It has been speculated that products of nano-joining often exhibit crystalline perfection at the joints due to the desire of the joined particles to rearrange to their lowest energy form - that is for the crystal orientation of both particles to match. Simulations done by [20] give the theoretical basis for this proposal using a molecular dynamic simulation, and measurements done in Chapter 3 corroborate this experimentally.

1.2 Project motivation

The nanobeams introduced in the Section 1.1.3 are new and never before characterized self-assembled silver structures. Because of the great many applications suggested and tried using nanobeams (see Section 1.1.1), finding simpler methods of creating them are necessary for advances in the field. These nanobeams are unique in that their fabrication did not require elaborate and expensive lithography equipment or chemical deposition. They were created in solution through a process of self-assembly, which is relatively cheap and efficient. It is imperative upon creation of novel nanostructures that they be characterized for quality assurance. By electrically characterizing material one can not only evaluate its use in electrical applications, but also gain deep knowledge regarding its physical structure. Resistivity measurement of these nanobeams in particular, serve as confirmation of the crystallinity of the product. If the structure is polycrystalline, *i.e.* it consists of different crystal grains, it will have resistivities much higher than single crystalline nanowires due to grain boundary scattering of transport electrons [22]. These grain boundaries would

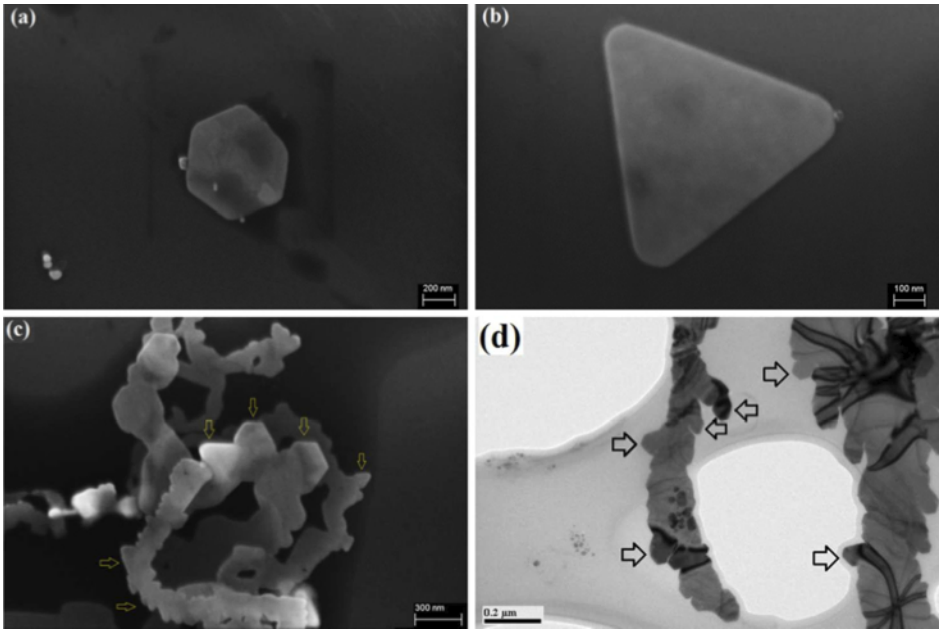

Figure 1.3: Images of a silver (a) hexagonal disk (b) triangular disk and (c) nanobeams assembled from hexagonal and triangular disks and (d) TEM image of nanobeams taken after construction (Reproduced with permission from [20])

be formed at the edge of the nanoplates where joining has occurred between two different crystal directions. If, however, the nanobeams turn out to be crystalline, the resistivity of the object must approach that of other characterized crystalline elongated nanostructures. To confirm this, the self-assembled nanobeams, are characterized in Chapter 3.

As the capability of nanotechnology to create smaller and smaller objects enhances, a major question becomes whether these small constituents can be joined together to make functional devices. Also, small devices are very hard to access and so welding them to larger structures for easier access can solve a major impediment. Due to the very good characteristics of polyol synthesized silver nanowires and the relative ease of their creation, these wires are prime candidates for use as plasmon and electron carriers. Finding a simple and reliable method of welding these nanowires that is flexible enough to be used in an industrial setting is imperative to the next generation of nanotechnological devices. For this reason we have invented a method of using Joule-heating to weld two polyol synthesized silver nanowires together, as explained in Chapter 4.

A central problem with the continued progress of nanotechnology in electrical devices is the existence of contact resistance. As devices get smaller the contact region shrinks

as well, causing contact resistance to go up. Contact resistance provides a source of noise [23] and can overshadow the desired response of the device. Other effects of contact resistance include undesirable power loss and excess heat. As such, there's a great demand for a welding technique that can reduce contact resistance to nano-sized devices without expensive equipment.

Another problem with contacts that is often ignored in discussion of contact resistance is the existence of electrically non-linear junctions. In particular, many contacts are not ohmic at the outset and display rectifying characteristics belonging to a Schottky diode [24]. In order to achieve desirable ohmic contacts, fabrication facilities go to great expense in ensuring a contamination free environment endowed with high vacuum pumps. In Chapters 4 and 5, a procedure is used to rid the contacts of the layer causing this behavior and achieve reliable ohmic contacts. These results can potentially save a great deal of cost associated with the extra care needed to ensure contacts are ohmic at the outset.

The next sections will go in depth in description of the current state of electrical nanocharacterization and nanowelding.

1.3 On the current state of characterization

1.3.1 Electrical access

The most pressing problem one faces when delving into the nanoscale is the difficulty and expense incurred in accessing structures at such small dimensions. In particular, applications like joining separate objects, physical manipulation, and electromagnetic stimulation are made ever more difficult by the small size scales in which such objects exists.

In this project, this problem is tackled head on and electrical access at the nano-scale is simplified, to be later used for characterizing and welding nanowires. In the past few decades since manipulation of nano-objects have become feasible, researchers have developed a myriad of methods to electronically access nanostructures. In the following sections several of these procedures will be explored, since understanding the field is necessary in explaining our choices.

Nanomanipulators

The most straightforward, yet one of the most difficult to execute methods of electrical access to nanowires is direct connection between the probes and the nanowires itself. Due to

the small and fragile nature of the nanowires a series of nanomanipulators is often required to achieve the accuracy in movement required to initiate contact [25]. In ref [25] the inner measuring probes were dug into the nanowire with a depth of 10nm to ensure good contact while two outer probes conducted current through the nanowire. Talin and coworkers [26] used piezo motors to achieve the accuracy required to contact the nanowires directly. Ref [27] uses a collinear equidistant 4 cantilever system of probes on chip, requiring only alignment before probes can be lowered into contact.

This approach however has multiple problems. In order to contact the nanowire directly, the probes have to be extremely thin and sharp. The creation of such probes requires elaborate nanofabrication techniques and the fragility of the probes makes transport difficult. The probes require microscope support, often in the form of a scanning electron microscope (SEM) or a transmission electron microscope (TEM) in vacuum, adding expensive equipment costs to the budget. Furthermore, the calibrating and placing of probes on the correct location without significant damage to the sample takes a great deal of time and cannot be implemented in a control system assembly line setting. Overall, using nanomanipulators to directly access nanostructures with probes is costly and is not feasible for industrial applications.

Electron beam lithography

Instead of directly probing the nanowires themselves, lithography, followed by deposition, can be used to fabricate metal electrodes on top of a nanowire. This allows a larger probe to probe the pads fabricated rather than the requirement for very small probes and microactuators. Electron beam lithography (EBL) is one of the most common methods of defining conducting electrodes on top of nanostructures. Using lithographic techniques as opposed to direct probing removes the need for sensitive probe actuators, and because the probes do not directly contact the nanostructure itself, this reduces damage. Depositing contacts also allows further or additional characterization to be done after the initial electrical measurement.

In order to remove the difficulties of direct probing, the eventual probe tip must have a large, clearly marked location for contact. This means that with lithographic techniques metal electrodes are often required to connect the nanowire to larger pads. Giving the probes a predesigned and relatively larger space for landing makes it possible to program probes to locate that spot and land with acceptable error, making assembly line implementation plausible.

EBL, like most other forms of lithography, requires a resist to transfer a pattern to.

An EBL machine (such as a Raith machine) marks the nanowire position and transfers the pattern onto the resist for the electrode-pad arrangement [1]. Due to the expensive equipment and maintenance costs however, this method is often altered. Goldberger and coworkers [28] used the much cheaper option of optical lithography to define the pads and mark the sample, and only used EBL to fabricate the electrodes connecting the nanowire to the pads.

With EBL, only one sample can be fabricated at a time, making the process extremely slow and expensive for creating a large number of samples. Furthermore, due to the vacuum requirement and the fact that nanowires are usually not seated in an ordered fashion on top of the substrate, assembly line mounting is very difficult to accomplish with EBL.

Focused particle beam deposition

Another common method of contacting nanowires is using a focused beam of particles, often a Focused Ion Beam (FIB) or a Focused Electron Beam (FEB), to direct a line of conducting material from the nanowire to a prefabricated set of pads. The process works by creating a source of ions/electrons, usually Ga^+ for FIB and filament electrons for FEB, which can be focused using electrostatic forces to strike a precursor gas already deposited on the substrate. The collision initiates a chemical reaction where the desired metal is deposited on the substrate while the other constituents evaporate in the form of a gas. This process is portrayed in the schematic in Figure 1.4. A high degree of accuracy can be achieved with this process as the principles of electrostatic lensing have been well understood for decades. A beam tip radius of 2nm can be achieved at the substrate with the smallest deposition dimensions known to be on the order of 10nm [29] for FIB and 0.7nm for FEB [30].

An example of this process being used to contact elongated nanostructures was illustrated by Liao and coworkers [31], where they fabricated pads using ultraviolet lithography and created electrodes, to connect the pads to the nanowires, using FIB. Similar procedures have been done [4, 32, 33] with various methodologies for creating the pads.

Hanratha and Korgel [34] compared the FIB, FEB and EBL processes for contacting germanium nanowires and found that due to ion milling, FIB is the only method of deposition that creates ohmic contacts at the outset. Ion milling however also damages the sample and forces impurities and defects into the structure being tested, possibly changing the properties. The scattering of the metal particles can also create various thin film segments around the substrate creating current leakage pathways that will compromise the accuracy of the product [35], also a problem associated with FEB. FIB and FEB also

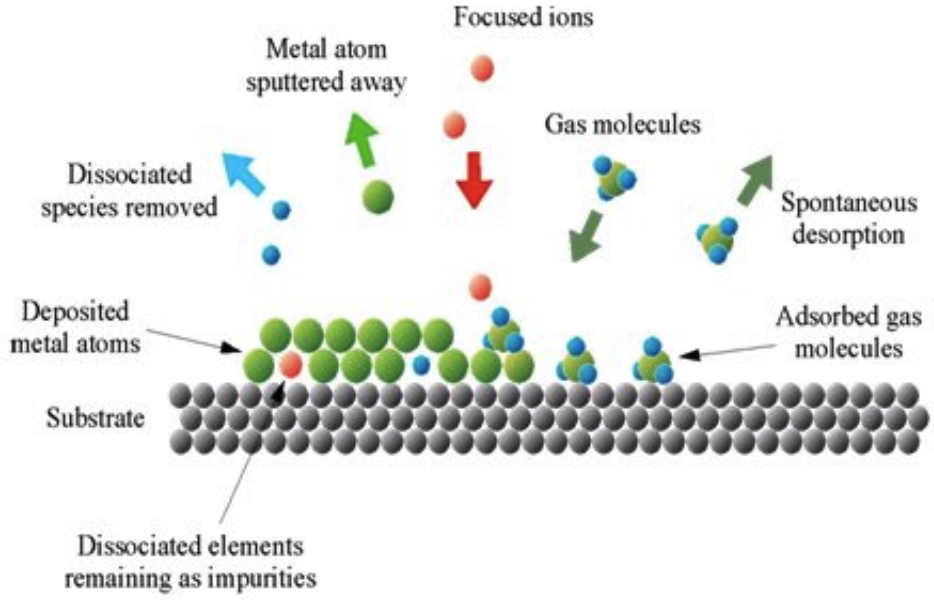

Figure 1.4: A schematic of the in process deposition of metal atoms using the FIB chemical vapor deposition technique (diagram taken from Wikipedia Commons)

require expensive vacuum technology, ion/electron guns and an accompanying SEM for visual confirmation. Furthermore, like EBL, FIB and FEB pattern one sample at a time, suffering from a slow process, and are also difficult to design into an assembly line control system.

Photolithography

Like EBL, photolithography involves the transfer of patterns to a resist on the substrate, except instead of electrons one uses ultraviolet light and most often a predesigned mask is used without the selectivity of a moving electron gun. Figure 1.5 shows an example of a device used in this project that was patterned in photoresist using a predesigned mask. Although once the mask is fabricated it cannot be changed, it provides the ability for quick fabrication of thousands of devices positioned in the same manner as the mask. Photolithography is often used to create the landing pads only, which are then connected to the nanowire with electrodes fabricated by a focused ion beam [36] or EBL [28]. However photolithography alone has also been used to contact nanowires directly.

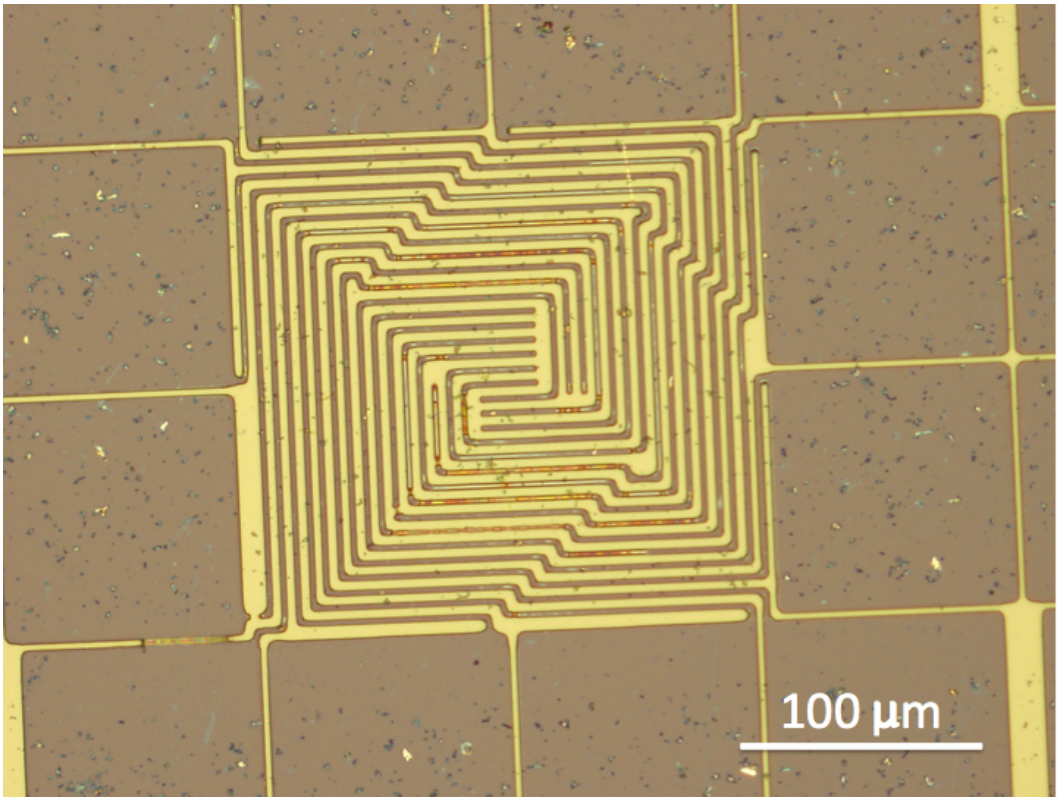

Figure 1.5: An example of a device fabricated in this project using photolithography in a Shipley 1811 resist. The trenches in the middle are not quite developed in some parts due to the resolution limit of photolithography resulted in problems exposing the sample.

One of the main problems with photolithography is the optical resolution limit. The lowest feature size achievable by optical printing without severe shape degradation is $f_{min} \approx \sqrt{k\lambda g}$, where k is a constant dependent on the photoresist, λ is the wavelength of light, and g is the distance between the mask and the photoresist. Experimentally, this limit comes to about 1 μm for exposure by a 400 nm wavelength mercury lamp source.

Due to these limits on resolution, two-point-probe is the most popular photolithographic characterization method [26, 7]. photolithography can also be used for 4-point-probe measurements [37, 38, 39], usually for structures at least 25 μm in length. The principles of two-point-probe and four-point-probe characterization will be explained in Sections 1.3.2 and 1.3.3 respectively.

To overcome some of the problems associated with photolithography, some researchers

have opted to modify the process. To solve the problem of selectivity, Parkinson and coworkers [40] used a direct-write laser apparatus to remove the need for a mask in their lithographic pattern transfer. The cost of the laser and actuators are now added, and the time spent is now similar to the EBL for patterning electrodes on each individual nanowire. This process however, unlike EBL, does not require expensive vacuum or SEM equipment.

The advantages of simple photolithography are mainly time and cost. Photolithography requires no vacuum technology and all components including the mask are common and economical. If one is able to create a sufficient number of devices per exposure, lithography can also prove to be the fastest of all the techniques in terms of the number of nanowires contacted per unit of time. Photolithographic processes have been mounted on assembly lines for years, particularly in the semiconductor industry. The downsides include the inability to guarantee successful electrode nanowire contact, the time required to find successful samples, resolution (depending on the number of electrodes the nanowires have a minimum length limit), and the reduced selectivity in contacting the right nanowire.

Overall this method of contacting nanowires was chosen due to the numerous advantages it provides. Since the nanowires welded and characterized in this project were all over 10 μm long, photolithography could be used for 2-point-probe measurement and welding on all of them. Furthermore, the nanowires that were characterized using the 4-point-probe measurement were on average 30-40 μm long, which is sufficient since our method requires only a 21 μm minimum nanowire length. With the resolution requirements out of the way, photolithography provided the fastest and most economical method for contacting nanowires. The mask was designed so that each patterning experiment provided close to a hundred probable devices, with minimal time spent. Our process provided for minimal damage to the nanowire and the contacts created were robust and required no extra care taken to preserve them. For these reasons photolithography was chosen over all the other methods.

1.3.2 2-point-probe theory

The simplest route to characterizing a material electrically is using the two-probe method. This method only requires current flow between two connections and the measurement of the voltage between the same probes. The main problem with two-point-probe measurements is the contact resistance caused by the change in shape, material and cross sectional area that occurs at the probe-material interface. This method is tolerable with bulk devices where contact area is large enough to mitigate surface scattering and bulk resistances are large enough relative the contact resistance. In smaller devices where contact cross

sections are within the μm range, the contact resistance becomes significant compared to the sample itself.

To remove the contact resistance or mitigate its effects, one can increase the contact cross section. Deposited metal films often grow in islands and the overlapped area does not represent the contact cross section. By heating the contact region, often by annealing as seen in [1, 28], one can increase the real contact cross section and reduce contact resistance. One can however avoid the situation all together by separating the voltage measurement and current driving probes. This method of measurement is called the 4-point-probe measurement.

1.3.3 4-point-probe theory

4-point-probe measurements, or Kelvin sensing named after Lord Kelvin for the invention of the Kelvin bridge in 1861, is a method of measuring low impedances using four points of reference. The original Kelvin bridge involved a configuration of resistors and there have been other methods of measurement proposed since. However, we concentrate here on the simple 4-point-probe method Chapters 3 and 5.

Suppose one needs to perform an impedance measurement of a material, where the resistance is on the order of the achievable contact resistance. With a regular 2-point-probe measurement, the resistance measured from an I-V curve would represent the material resistance added to the two contact resistances. With four probes the situation is different. Call the 4 contact resistances $R_{c1,2,3,4}$ and suppose the two outer probes are connected to a current source while the middle probes are connected to a voltmeter. In this situation since we are working with a semiconductor analyzer each probe must act as source or ground on its own. The schematic drawn in Figure 1.6 shows the probe scheme of the probe station on the left.

Assuming that the electrodes have no effect on voltage, the voltage is constant at the boundary points, and the wire is uniform, the electric field is then uniform within the wire [41]. Since the nanowire is very thin one can assume that at the boundary points, *i.e.* at the electrodes at the ends, the voltage is nearly constant across the nanowire cross-section. The polyol synthesized pentagonal cross-section nanowires are atomically smooth and so have a uniform cross-section along the wire axis, however the nanobeams tested in Chapter 3 do not. One can approximate the nanobeams to be smooth since changes in beam diameter are small compared to the distance between the probes. Having met the requirements for a uniform electric field, one can then model the configuration as an idealized circuit model as in Figure 1.6 on the right side. If one assumes that the voltmeter

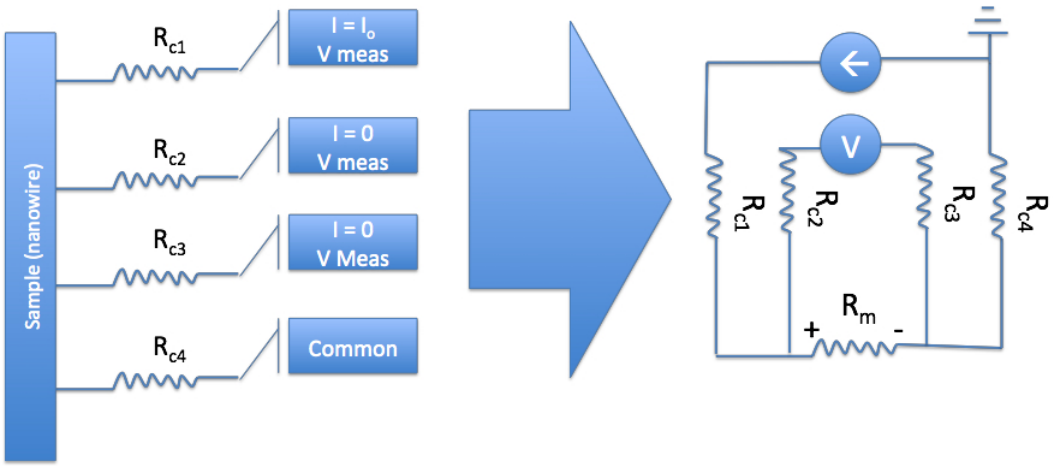

Figure 1.6: The schematic of how the 4-point-probe apparatus can be idealized in circuit form. The R_cs represent the contact resistances of the respective electrodes, while R_m represents the measured resistance of the sample between electrodes 2 and 3.

and the current source are idealized, the idealized source keeps the current at a constant regardless of the contact resistances attached to it and the voltmeter has infinite resistance so no current enters the inner loop. The contact resistances are thus rendered irrelevant. Then $R_m = \frac{V}{I}$, with $V = V_2 - V_3$ and $I = I_o$ with I_o representing the forcing current and V_n representing the voltage at electrode n. The resistivity can then be calculated using the dimensions of the wire between the two middle probes by using the equation $\rho = \frac{RA}{l}$ where A is the cross sectional area, and l the length between the two electrodes.

Although these idealizations are often not precisely accurate they are none-the-less viable approximations. Most nanowires are atomically smooth and due to their cross-sectional size there is no significant variation in voltage along the diameter of the wire. Even for our larger non-uniform-surfaced nanobeams, like the ones characterized in Chapter 3, the variations in nanowire voltage will not be so great due to the small size of the nanobeam. Therefore the measurements done on these beams will be accurate within less than an order of magnitude.

1.4 On the current state of nano-welding

A fundamental problem associated with constructing complex nanosystems and devices is creating a procedure for secure welding and connection of smaller synthesizable parts.

This has applications in nanoelectromechanical systems (NEMS) for connecting moving parts and packaging [42] and could also have a fundamental role to play for nanoelectrical devices in creating electrical interconnects [43]. Nanowire welding in particular has found uses in surface plasmon carriers [44], nanoelectromechanical resonators [45], nanowire metal/semiconductor heterostructures [46], and p-n junctions [3]

To this end, researchers have invented a variety of ways to weld small structures. Like electrical characterization, the main problem with welding nanowires is accessing the small dimensions. Clever methods have been invented, from self-assembly to using light, to initiate reliable welds at the nanoscale.

1.4.1 Diffusion nanobonding

One of the most promising solutions to the problems of accurate manipulation and fast construction in nanotechnology is self-assembly. Self-assembly refers to the organization of discrete components into a coherent body as a result of interactions with the environment. In nanotechnology self-assembly is used for the creation of complex nanostructures by situating constituents such that a reduction in energy can be achieved by the constituents joining. In particular diffusion nanobonding occurs when suitable conditions are created for the surface atoms of one constituent to travel across to the other, joining the particles in the process.

Diffusion nanobonding has been used for the purpose of constructing a variety of different structures in past two decades. Li and coworkers [47] assembled barium chromate nanostructures such as threads and super lattices, while Tang *et. al.* [48] joined CdTe nanoparticles to create nanowires with interesting optical properties. Murphy and coworkers [49] successfully fused gold and silver particles to create nanorods with high aspect ratios. The particles were capped with a specific surface group, which allowed the joining of particles along the axis, creating longer and longer structures. This method is the most common route for fusing particles into anisotropic structures and is graphically elaborated in Figure 1.7. The process was done entirely at room temperature and produced gold nanorods with aspect ratios of up to 25 and silver nanorods with aspect ratios of up to 400. Nearly all joining experiments above reported crystalline behavior from the fused end-product.

This process can also be used to fuse already synthesized elongated structures. Carbon nanotubes have been welded to Ti electrodes under ultrasonication, greatly reducing contact resistance and improving performance [50]. By bringing clean surfaces of two

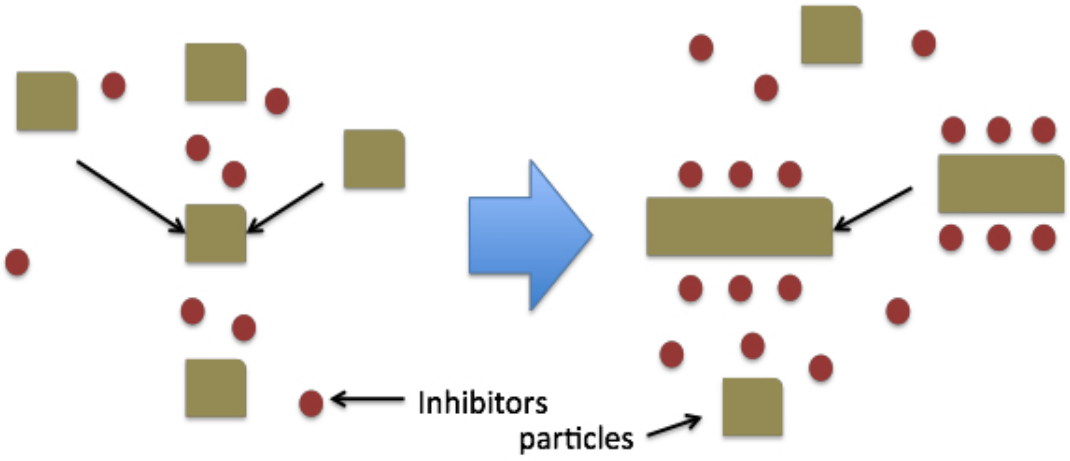

Figure 1.7: A cartoon diagram of particles (gold box) and inhibitor molecules (red circles) and the interactions inside solution. The inhibitor molecules attach to all but one dimension of the particles, allowing for joining in that direction.

nanowires in contact, initiating a crystal realignment and diffusion, researchers have cold welded gold[51] and silver [52] nanowires to create a single elongated structure.

The conditions required for diffusion nanobonding are often not satisfied (clean surface, contact at the ideal location, etc.) and very little has been shown in terms of welding different types of materials together. To my knowledge the welding region has not yet been tested for electrical or optical transport properties.

1.4.2 Soldering

Welding using soldering at the nanoscale is similar in principle to the bulk version, where a sacrificial material is required to make a reliable weld. However, at small scales the delivery of a sacrificial layer to the desired location is challenging.

Peng and coworkers used nanomanipulators retrofitted within an SEM to mechanically transport a sacrificial SnAu nanowire for welding two completely different wires [53]. In another experiment, graphene was connected with various materials using a micromanipulator probe tip and In as solder [54]. Gu and coworkers fabricated the solder material right at the nanowire tip, making heat the only requirement for ohmic joining of two nanowires touching end to end [55].

Soldering, like cold fusion above, requires an extra contact step for electrical utilization

of the finished product, for example p-n junctions. Furthermore relocating the sacrificial layer to the correct position requires precision movement, prefabrication, and often, an added variable of chance.

1.4.3 Pulsed laser welding

A more recent method of welding solids together uses ultrashort (< 1ps) laser pulses. Using this method one can excite the atoms of the sample surface faster than the electron-lattice thermal coupling time (> 1ps). The exact details of the laser pulse matter interactions are investigated by Linde and coworkers [56]. Simply put, the laser prods the chemical bonds on the surface of the structure, making it more volatile and ready to diffuse. This leads to the restructuring and bonding of structures in close vicinity. Kim and Jang [57] used this method to weld gold nanoparticles, initiating a reliable weld with weld characteristics similar to that of Joule-heat induced welded Pt nanowires [19].

1.4.4 Miscellaneous

Other less common methods such as welding by scanning probe microscopy (SPM) [58], high intensity electron beam [59], ion irradiation [60], hydrogen welding [61], and Li-assisted electrochemical welding [62], have been suggested and implemented. These methods however do not have the clout with researchers that the methods discussed in detail above do. This is often due to limits with long term, sustainable applicability such as with hydrogen or Li-assisted welding, where rare material is needed. SPM welding, ion radiation, and electron radiation are expensive and have no in-experiment method of knowing when the weld is completed for each wire without additional resources, and thus can easily damage wires.

1.4.5 Fusion welding

Plasmonic welding and Joule-heat welding are both subsets of a common method of welding called fusion welding. Fusion welding entails the joining of two structures by melting the surfaces closest to each other to facilitate atomic diffusion. This can lead to atomic bonding or alloying at the interface, where often a combination of the two materials is present, holding the two devices together. Light-induced and Joule-heat welding are very popular among researchers due to the ease of equipment access and relatively low cost.

Both procedures can be completed in air and can potentially be easily mountable on an assembly line.

A study on plasmonic welding was done by Garnet and coworkers in 2012 [63]. In this paper, pentagonally-twinned polyol process silver nanowire meshes were deposited on a silicon nitride membrane and were exposed to a broadband tungsten halogen lamp for 10-120 s. In contrasting the plasmonic weld method with the other methods, they showed that due to conglomeration of plasmons at the junctions, the heating was mainly concentrated there. Furthermore, they showed that as the two nanowires welded, the plasmon concentration decreased, leading to a self-limiting weld. Performing the same experiment with hot plates they found that due to the lack of selectivity, the point at which junctions welded was very difficult to determine and the mesh either remained unchanged or was destroyed. Spechler and Arnold [64] used nanosecond long laser pulses to weld a nanowire mesh also for reduction of surface resistance. Since the laser pulse duration is not below 1 ps, this experiment is considered one in fusion welding, as heat is involved (refer to Section 1.4.3 for pulsed laser welding).

Joule-heat welding requires that the mechanism for melting the surface of the nanowire be electrical resistive heating. Bundles of single walled carbon nanotubes have been welded together inside a transmission electron microscope using a tungsten tip at a voltage bias of 2 V [65]. More recently, Tomyoh and coworkers [19] investigated the structure of Joule-heat induced welding in Pt nanowires and found that the weld had the same resistivity as the nanowires themselves and that the weld region had a very thin profile. Tomyoh also showed in 2009 that with Joule-heating, most of the heat is concentrated at the contacts and at the center of the nanowire lengths [18]. He showed that an energy band exists where the contacts are sufficiently heated for welding without destroying the center of the wire itself.

There have also been reported uses of the Joule-heating method in improving the contact between nanostructures and electrodes. Dong and coworkers [66] studied the effects of Joule-heating on reducing the contact resistance between carbon nanotubes and gold electrodes, finding that the contact resistance can be reduced by nearly 30%. Yu and Yan-Guo [67, 68] performed a series of experiments inducing pulsed currents through a gold contact into a ZnSe semiconducting nanowire. They reported successful welding of a nanowire to the electrode and the elimination of the Schottky barrier between the wire and the metal.

Joule-heat welding of pentagonal cross-section polyol silver nanowires to each other is investigated in Chapter 4. Our method uses photolithography to pattern pads between which two nanowires are situated in series. By probing the pads using regular probes, electrical current is forced through, which welds the nanowires through Joule-heating. The

ease by which photolithography can be used to pattern the pads used for probing the nanowires and the ability to create hundreds of devices per sample make our method very attractive. Furthermore a novel process is invented to destroy intermediate layers and achieve a reliable weld quickly without destroying the nanowires.

In Chapter 5, the same process of photolithography coupled with Joule-heating is used to weld nanowires to the contacts to reduce contact resistance. The method used to weld the nanowires, unlike other such attempts [67, 68, 66], does not use pulse currents or complicated current sources. Here instead, a common semiconductor analyzer with ramp sweep capabilities is used, with the added advantage of being able to recognize a weld and measure resistance right away.

1.5 Organization of thesis

This thesis is regarding the creation of novel techniques for investigating and altering the electrical properties of metallic nanostructures, in particular elongated structures such as nanowires and nanobeams. Chapter 2 contains information on the methods designed to probe these devices and the choices made will be explained. In Chapters 3, 4 and 5, three novel applications of our procedures will be explored. Namely the electrical characterization of a novel nanomaterial, investigating the welding of two never before welded nanowires, and using Joule-heating to reduce contact resistance with commercially-bought nanowires, respectively.

Chapter 2

Fabrication of contacts for individual nanowires

The first challenge one may face in investigating the electrical response of objects with dimensions less than 10 μm is the expense incurred in small tip diameters and micro-actuators that would be required to directly contact these objects. Furthermore, high microscope resolution may be required which can get quite costly as one moves from an optical microscope to a SEM. As the title of this thesis suggests we will focus on simple and economical methods for achieving our ends.

To this end the solution then lies in creating successive steps of connections whereby the nano-sized object can be attached to a slightly larger device that can successively be attached to a larger device, and so on, until the final device is in the size scale of cheap, easily available probes. The metal pieces directly connected to the nanostructures being tested will be referred to as electrodes, and the landing blocks made for probes will be called pads. To achieve this step, one must design the electrodes and pads first and somehow connect them to the object being probed

2.1 Choosing a method

There are many methods of contacting the nanowires and the nanobeams that we will investigate in this project, and a great bulk of them are explored and discussed in Chapter 1. Although some of these procedures might intuitively feel like the first choice, this may

be a deception. Thus a full discussion of our top choices and the process in choosing a methodology is warranted.

Methods such as using micro-actuators [18], or using ultrathin probes [25] have been employed by other researchers. For this project however the most economical and easy to utilize solutions to accessing the nanowires are desired. For our research the purchase of high precision probes and microactuators combined with the required scanning electron microscope (SEM) time would have been rather costly. Furthermore, a method of mass fabrication would suite industry needs much more aptly, and would allow us more room for error. For this reason the procedure of direct probing was rejected and an electrode fabrication method was chosen instead.

As discussed in Chapter 1, the most common method used for fabricating electrodes is electron beam lithography (EBL). With this method each device requires calibration for positioning and must be done on an individual basis, substantially decreasing the availability of devices. Furthermore, the electron beam causes local heating in the nanowire and can cause structural changes to the wire [34, 35]. Furthermore, as mentioned before the cost of per hour use of EBL equipment is rather steep and is not feasible for this type of research.

Another common method used for contacting small objects, uses what is called focused ion beam (FIB)[35]. The intricacies of the FIB method is discussed in detail in Chapter 1. Pads can be fabricated using any other method such as EBL and photolithography and connected to the nanowire using FIB. The drawbacks mentioned above for EBL also largely affect FIB, including the price and positioning calibration. Due to the large size and the striking force of the Ga^+ ions, the resulting momentum of the particles is large enough to often destroy both the substrate and the device. Furthermore, the ions are easily embedded into the specimen, which can dramatically change the structure and properties of the object being probed. On top of that, the FIB machinery is not always found in common fabrication facilities. Damage to the sample, restricted access, and cost are the reasons why this method was not chosen

Our proposition is instead to use simple photolithography with modifications to make it a viable contender. Nanowires in solution are first distributed over the sub- strate as evenly as possible and predesigned devices are be fabricated on top. Because the nanowires are in random positions, and orientations, an optical microscope must be used to find devices with nanowires situated in proper positions. Since nanowire lengths tested in this project mostly exceed 4 μm, common photolithography, capable of a minimum feature size of 2 μm, can be readily utilized with a single step to create the required interconnects. To make photolithography advantageous in terms of cost and time, devices must be closely packed

so that as many nanowires as possible are contacted per a unit of area on the substrate surface. Furthermore, the capacity for device error must be diminished so that as many fabricated samples can bear fruit as possible. With that, the design of a photolithorgraphy mask becomes our next step.

2.2 Mask design

The following points summarize what a designer must keep in mind while drafting the photolithography mask:

- To avoid the cost of creating multiple masks, the ideal design would contain all successive devices from the electrodes contacting the sample, to the probing pads in a single pattern
- No feature of the mask may be lower than the photolithography feature size minimum of 2 μm
- Taking a Cascade Microtech® DC parametric probe as the standard would require a minimum 30 μmx30 μm pad suitable for probing.
- Due to the non-selective nature of photolithography, one would prefer to keep the pad-to-electrode (hereby also referred to as fingers) ratio to a minimum to maximize the amount of nanowires contacted. Devices must be designed such that they can be packed closely together without compromising patterning quality
- Fingers that are too long on the other hand can create a danger of more than one nanowire being contacted causing shortage and uncertainty in the data
- Fingers must be thin enough so that a 4-point-probe measurement is possible on a reasonable percentage of randomly oriented nanowires on the substrate. In other words if fingers are 3 μm thick and 3 μm apart from each other a 4-point-probe measurement can only be done on nanowires 21 μm long and perfectly aligned, perpendicular to the fingers.
- Since multiple tools with multiple lab locations are needed to find, check, probe and recheck the nanowires, a mapping system must be designed to track the nanowires previously found. The mask is first divided into several different sections for each type of device. Each section is further divided into subsections, named brigades,

marked with a letter across and numbers vertically. Each brigade contains a known number of devices and can be mapped thus. Refer to Figure 2.1.

- And finally, multiple devices can be put on the mask since as Richard Feynman famously stated: "there's plenty of room at the bottom"

In an attempt to reduce costs further a free drafting program was sought out. A windows compliant freeware called LASI (LAyout System for Individuals) version 7 was used to draft the mask and convert the file to GDS format. This is the format required by most mask manufacturers. The mask was ordered and created by The Photoplot Store, located in Colorado, U.S.A.

The following are some of the devices designed on LASI7 and included as part of the mask used for the lithography process:

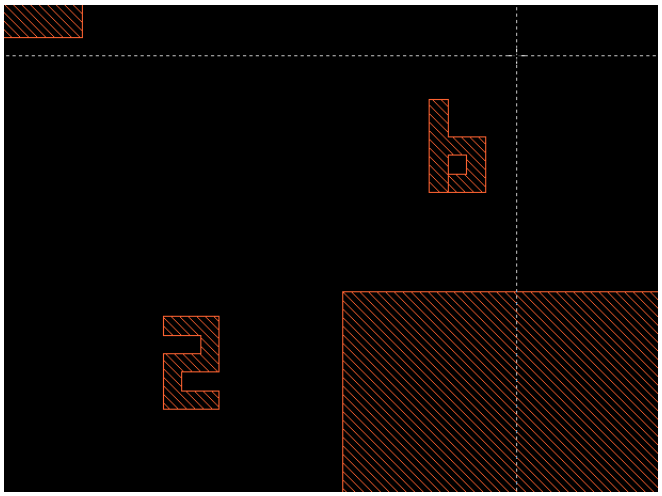

Figure 2.1: The devices were grouped into brigades of 10x10 or 20x20 with each group being a part of the larger coalition of similar devices put in a section of the mask. Each brigade is identified with a letter horizontally and a number vertically, creating a mapping system for easily identifying devices. A typical map of a device is indicated by for e.g. (Z,5)(4,9), where the former bracket represents the location of the brigade and the latter bracket represents the row and column number of the specific device.

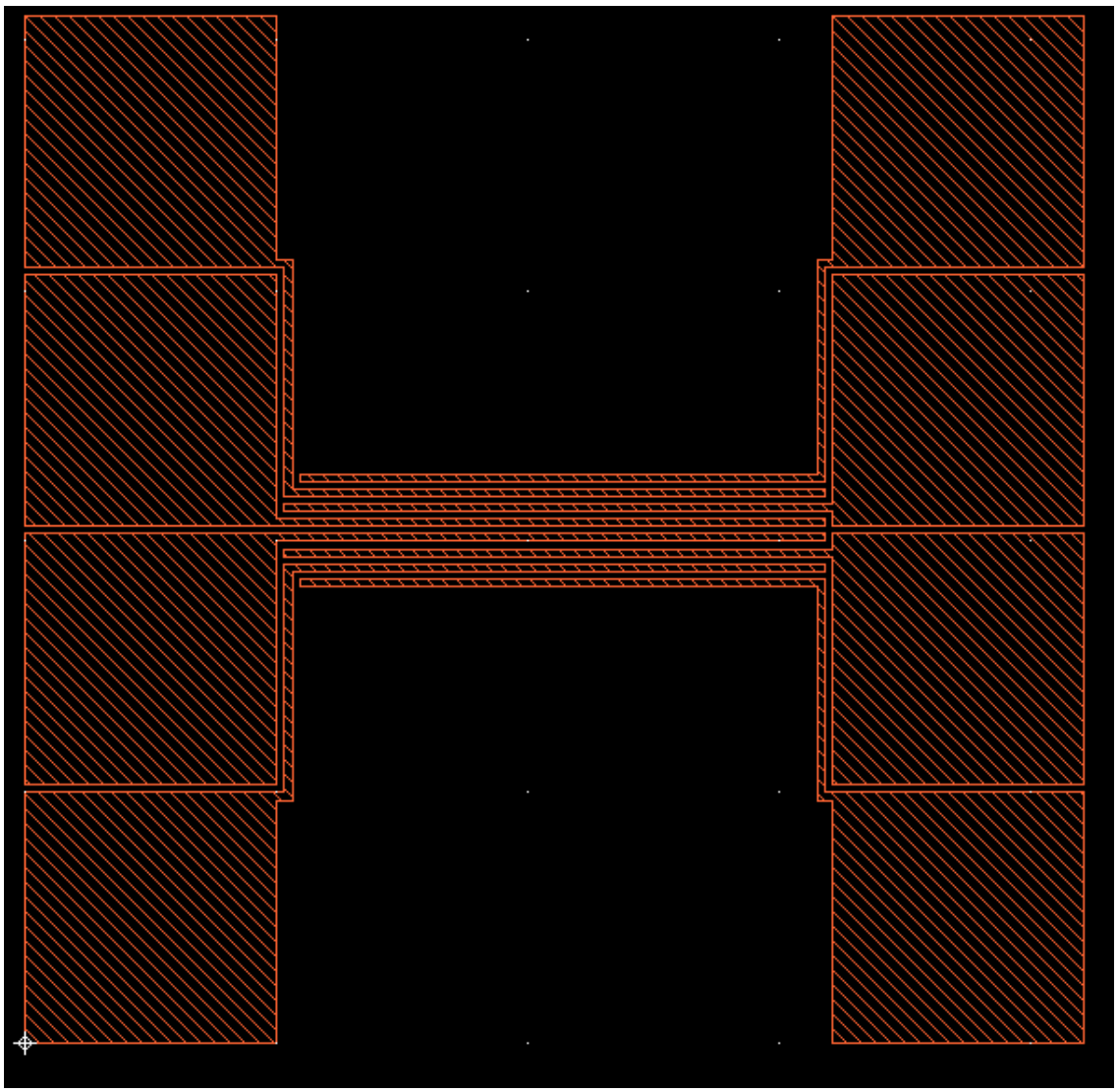

Figure 2.2: The Finger Pattern is the simplest creation for 4-point-probe measurements. The fingers extending out of probeable 100 μm by 100 μm pads, are themselves 3 μm thick and 200 μm long. The finger area to pad area ratio of this device is 0.133. This is a central device in probing high aspect ratio devices.

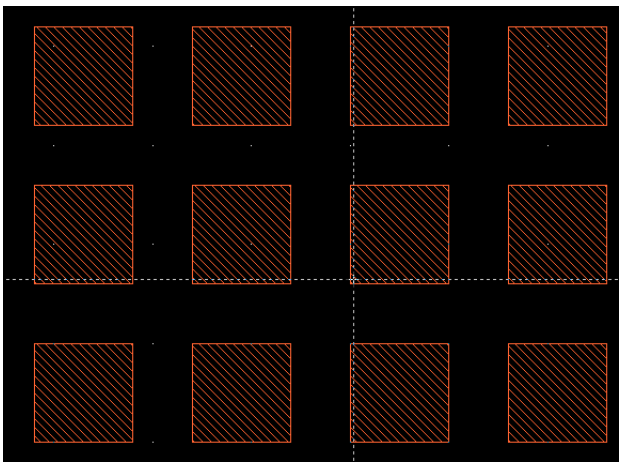

Figure 2.3: Another central device in investigating nanowires is the pad array. A pad array is an easily fabricated array of 100 μm by 100 μm pads that can connect directly to two sides of a device, making 2-point probe measurements extremely easy and efficient. There are three battalions of pads with separation sizes of 4 μm, 20 μm and 40 μm on the mask.

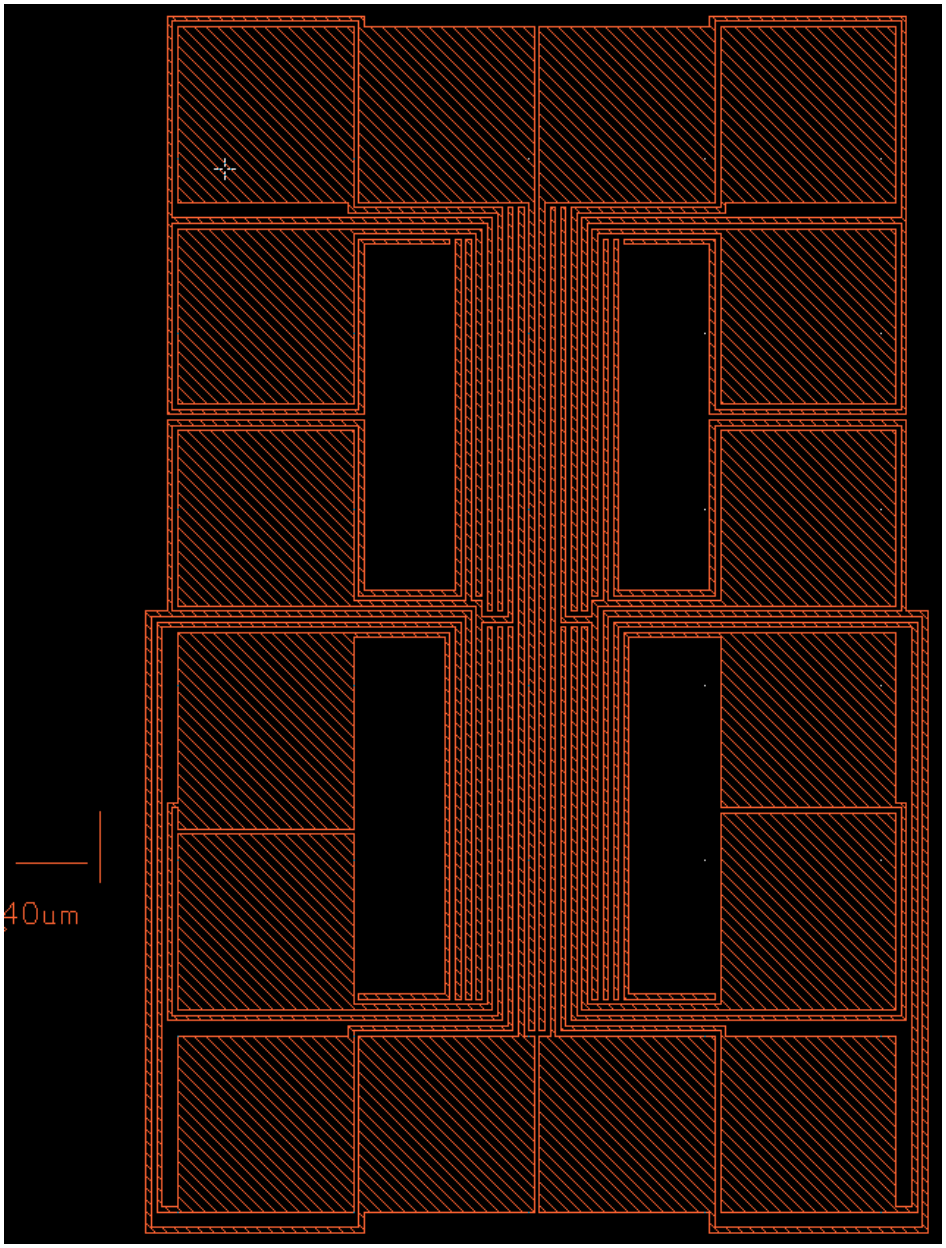

Figure 2.4: An example of a pattern invented to increase finger-area to pad-area ratio; this pattern has a ratio of 0.2. In the end however fabrication proved difficult and long fingers proved disastrous with silver particles shorting the electrode. For these reasons the design was never utilized

2.3 Centrifugation

The procedures used for synthesis of the particles investigated in this thesis, as described in Chapter 1, leave as a byproduct small and medium sized silver particles inside the solution. No better example of this than the method used to create the nanobeams tested in Chapter 3 [20]. The process used to create the beams leaves behind hexagonal and triangular plates, and clusters of nanobeams joined together(*i.e.* junk). Since the junk size often reaches 6 μm in diameter, it will surely interfere with devices designed in the previous section if in large enough concentrations(refer to Figure 2.5).

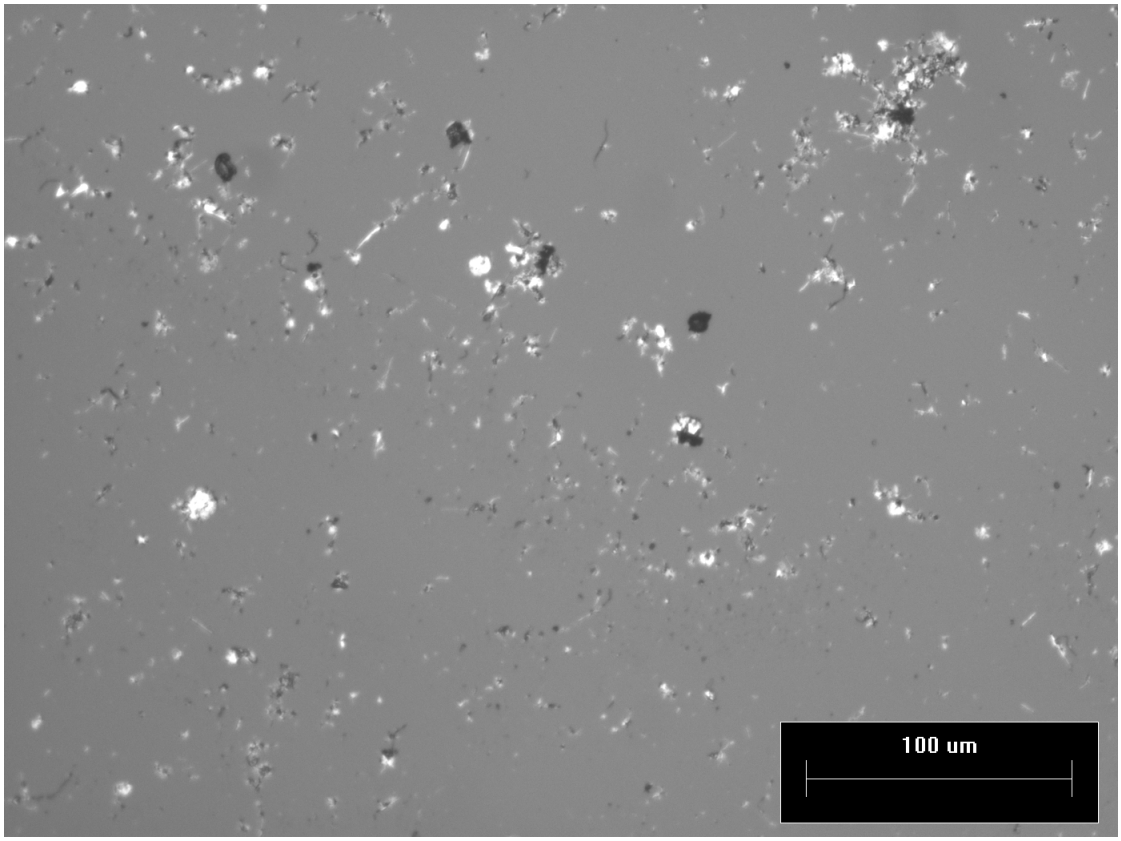

Figure 2.5: This is an example of post reaction solution. It is clear that nanobeams are by no means the only particle in the solution.

To separate the desired particles from the by-products of the reaction, a method of centrifugation was employed. The process gets its name from centrifugal force, which is applied to any object under rotation. However, any force applied to the solution, including

gravity, is sufficient to perform centrifugation. All particles in solution under a force greater than the fluid pressure from below will accelerate, and moving particles in fluids are subject to a drag force:

$$F = \frac{1}{2}\rho v^2 C_D A \tag{2.1}$$

Where ρ is the density of the fluid, v is the velocity of the particle, C_D is the drag coefficient, and A is the cross sectional area of the particle. Equation 2.1 makes it clear that different particles within the solution will travel at different rates within the fluid if a downward force is applied.

The samples used in Chapter 3 were cleansed using gravitation as the accelerating force applied to the particles with the longest nanobeams precipitating at the bottom within 2.5 hours of agitation and smaller particles remaining afloat.

The samples used in Chapter 4 were cleansed using a centrifugation machine. The sample was drained at the halfway point of the liquid column several times after 3-4 minute long spin recipes spinning at 1800-2000 rpm. The images of the cleansed and uncleansed samples are shown in Figure 2.6.

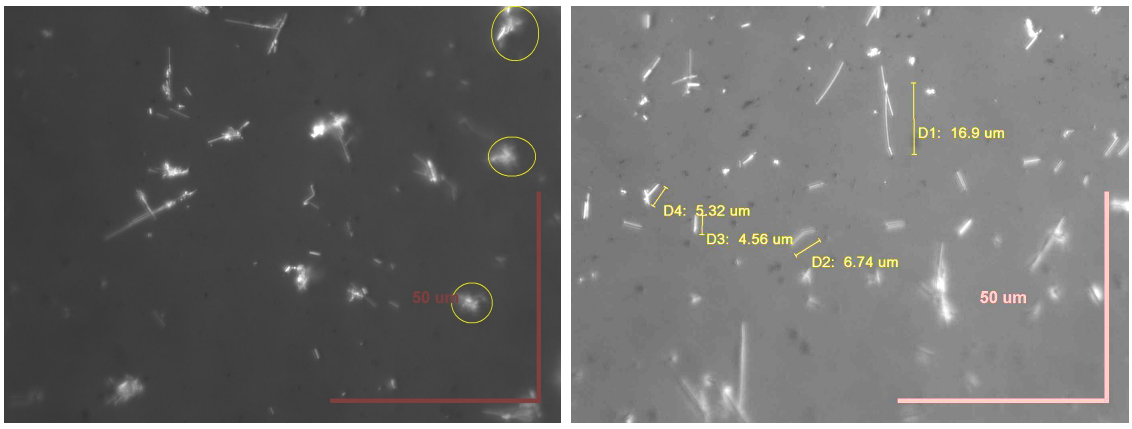

Figure 2.6: The comparison between optical microscope images of uncleansed (left) and cleansed (right) samples. The solution on the left contains large silver particles that are removed during the centrifugation.

2.4 Nanowire deposition and polymer removal

2.4.1 Deposition

Deposition of nanowires entails what is referred to as drop casting. Agitated solutions of the wires suspended in a liquid are pipetted on a wafer surface, awaiting evaporation. Once the sample dries, the precipitates of the sample, *i.e.* the nanostructures, remain on the surface.

The main issue with this step is the dispersion level of the wires on the sample surface. The wires must be as spread out as evenly as possible, so that the electrodes have the best chance of contacting a single nanowire, with minimum possibility of another nanowire shorting the line. The agitation of the solution is key to achieving a suspended solution without any particles sticking together, and since sonication causes the nanobeams to break, one must shake the solution by hand for several minutes. Furthermore, the particles also tend to aggregate on the surface of the deposited drop due to surface tension, while the drop dries. The result of this is that the precipitate left over on the surface, rather than being a dispersed field of particles, turns into clusters of inaccessible conglomerated wires. Figure 2.7 shows an optical image of precipitated silver particle clusters on a Si sample. This is also the reason why it is recommended that the solvent be a high vapor pressure liquid with low surface tension, so that the drop spreads on the substrate surface and evaporates before conglomeration can occur on the drop surface. Another solution is to apply gentle flowing air (preferably nitrogen) to the sample as the liquid dries. This agitates the drop of liquid causing its surface particles to move inside the liquid, for the liquid to dry faster, and for the liquid to spread out as thin as possible, which causes the landing of nanostructures on substrate surface easier. A combination of all these techniques were used for all samples drop casted in this project.

Once the method is chosen, one has to plan the orientation of the devices with respect to each other and the order by which they are deposited. The order, it was decided, is to have the nanowires on the bottom and the deposited electrodes on top. The first reason for this is to avoid the formation of a surface adsorbate on the electrodes, that would form an extra layer of insulation between the nanoparticles and the electrodes [37, 69]. The nanowire is already covered in a layer of insulation (PVP) and depositing the wires first allows for the removal of the polymer before electrode deposition, making direct contact more likely. Furthermore, the well created in between the pads can cause the bending of nanowires bridging the gap on the surface of the pads. This bending not only reduces the contact region, due to the wire ends lifting, but cracks in the wires have been reported[70].

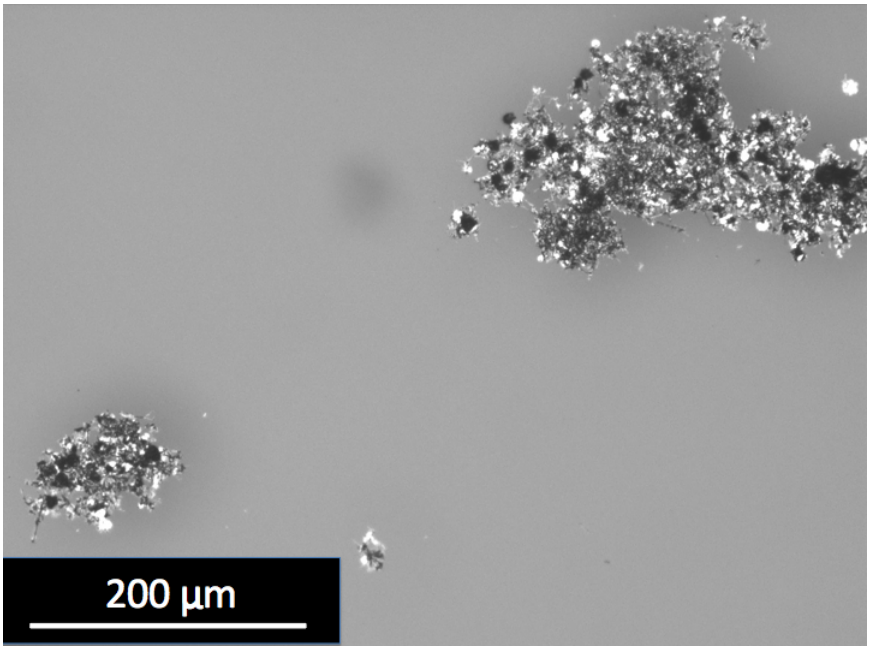

Figure 2.7: an example of clustered silver particles on a Si sample. To reduce this type of conglomeration in the precipitated sample the measures discussed in 2.4.1 are taken

2.4.2 Polymer removal

As discussed previously, the nanobeams are synthesized using the polyol method. The result is that the nanostructures produced will be covered in the polymer Polyvinylpyrrolidone(PVP), which hinders electrical connections to the particles. In order to make good electrical contacts to the nanobeams, one has to remove the polymer layer. Two common methods used in this project will be discussed.

The first one is to anneal the nanostructures, which burns the PVP off of the samples, before fabricating the required contacts. This method requires heating the substrate after deposition at 250^{o}C for 30 minutes. This is, however, not feasible for temperature sensitive samples and has been shown to not work quite as effectively as the second method [71].

The second method is to use a solvent such as acetone or ethanol to dissolve the PVP off of the nanostructures once the deposition is complete. This method is less damaging to the wire structures and relinquishes the requirement for an oven.

2.5 Selection of substrate and fabrication materials

The wafer was selected to compliment our stated purpose of availability and to suit the need for a substrate that insulates the devices and is capable of resisting run off currents. The obvious choice was a silicon wafer with a 150nm of SiO_2 deposited on top. The wafers are cheap and easily available from any major nanotechnology supplier.

If the nanowires are to be deposited first and electrodes second, it necessarily means that the nanowires must be taken through a photolithography fabrication process without major structure changes. Although it is ascertained that the major tools of photolithography do not affect silver to a noticeable extent, it is worth mentioning that certain cleaning tools could not be used, and major agitation such as sonication had to be avoided at all costs to avoid the breaking of the nanowires. Also with the photoresist being developed on top of the nanowires, there is always a risk of left over resist insulating the nanowires from the electrodes. Furthermore, major heating above 120^oC for prolonged periods of time needs to be avoided.

As for the choice of electrodes, the most common metal used for such experiments, gold, was found to also be the right choice for us. Although much more costly than other metals, gold presents properties that are ideal for experiments involving electrical conductance. With high conductivity and potential for silver alloying (better adhesion and electrical connection), gold is also one of the least reactive metals, precluding the potential for oxidation and electrical insulation[72].

2.6 Fabrication process

All fabrication for this project was performed at the Quantum Nano Center fabrication facility at the University of Waterloo.

Like most standard photolithographic processes on SiO_2, this process begins with a hexamethyldisilazane (HMDS) vapor deposition to render the surface more hydrophobic to enhance the acceptance of the subsequent photoresist spin. HMDS is applied using the YES HMDS Oven at 120^oC.

The first layer of photoresist used, polydimethylglutarimide (PMGI), is spun on the samples using a standard spin coater and baked at 140^oC. The second photoresist, Shipley Microposit 1811/1805 (depending on availability), is spun using the same methodology on top of the PMGI layer and then baked at 110^oC.

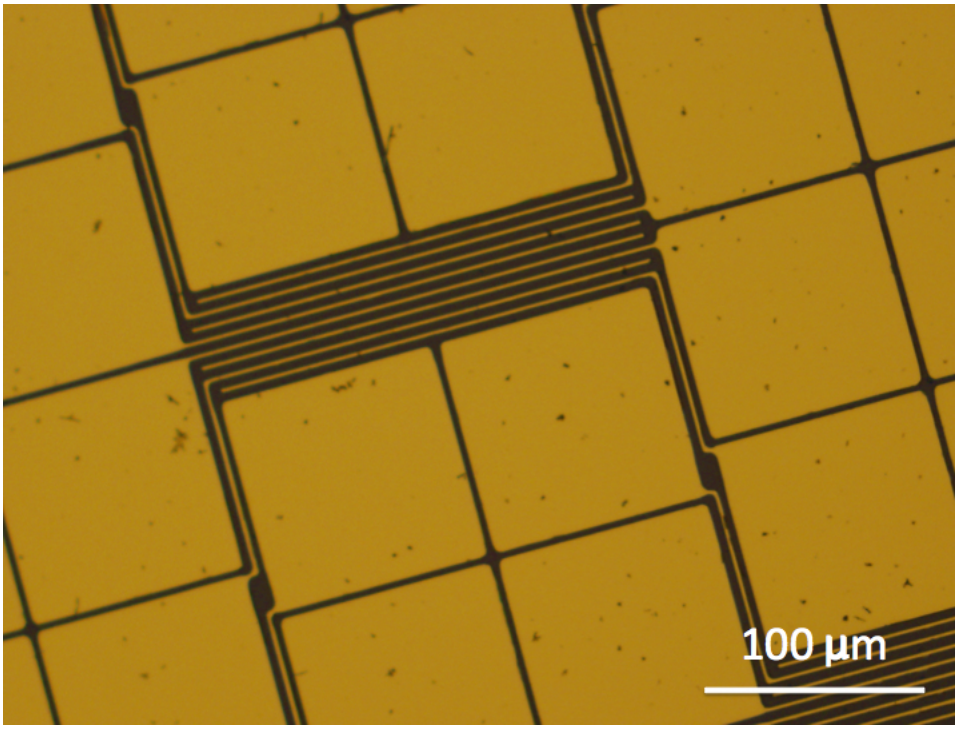

Figure 2.8: The final device fabricated using the process described in 2.6

The bilayer of resists is critical to the lift-off process due to the fragile nature of the nanowires; the nanowires cannot be subjected to sonication or other major turbulence as discussed before. Due to the difference in developing rates of the two layers of photoresist, the profile of the created pattern forms the sidewall profile of a thicker top and a thinner bottom, or the "T profile". The bilayer then allows the solvent to penetrate underneath, due to poor gold step coverage, completing the lift-off process without major agitation.

The photoresist is then exposed using an MA6 aligner and the mask designed in section 2.2. Shipley MF-319 was used as the sole developer.

A 60-80 nm layer of Au was then deposited with a 5-10 nm adhesion layer of Ti below. It is well known that gold does not effectively bond to SiO_2 and the titanium layer prevents flaking of the electrodes off the surface of the substrate.

The lift-off process was performed using the solvent PG Remover with very mild agitation of the samples inside the solution. A sample of the final product is displayed in Figure 2.8.

2.7 Probing

All probing of the samples was performed at the Giga to Nano (G2N) laboratory at the University of Waterloo with a Cascade Microtech probe air table and an Agilent 4155C Semiconductor Analyzer as the spectrometer (hereby referred to as the Probe Station). All SEM was performed either at WATLAB or G2N at the University of Waterloo.

Suitable wires, that is nanowires situated to be in contact with the required electrodes, were found using an optical microscope capable of viewing with a resolution of 0.1 μm. The locations of trapped nanostructures were recorded for later use and then later found for probing using the mapping system shown in Figure 2.1.

Once sufficient nanowires were detected on the optical microscope, the devices would then be viewed under the SEM, to ensure the nanowires were whole and connections were intact. This is to track any changes in the nanowires through the proving process and to reduce a potentially large amount of time spent on the probe station attempting to connect to nanowires that are physically disconnected. Using an optical microscope to initially find the nanowires further reduces the cost by eliminating the time spent locating the wires using the more costly SEM.

Chapter 3

Electrical transport measurement of Ag nanobeams

3.1 Why nanobeams

In this chapter, novel, never before tested nanomaterials are electrically characterized using the electrode fabrication methods discuss in Chapter 2. In particular, novel silver nanobeams have been synthesized and their investigation may shed light on the mechanism by which particles nanobond.

These nanobeams are created by diffusion nanobonding, or cold welding, of individual hexagonal and triangular silver nanoplates. The procedure for the creation of these nanodisks and subsequently the nanobeams is explained in detail in Chapter 1. Polymer inhibitors are used to ensure the plates only join at the edges and not the faces, making the cross section of the nanobeams rectangular. Silver nanobeams may posses interesting characteristics. For example, nanoparticles of different sizes and shapes display different electromagnetic interaction characteristics such as plasmon resonance frequencies [8]. Using this tunability one can create accurate sensors where the specific frequency of incoming electromagnetic waves can be detected. For this reason it is important to invent and understand different types of nanostructures for future use.

Since these nanobeams are created through a random joining process, they are expected to be polycrystalline, due to grain boundaries that would form along the connection between individual nanodisks. However computer models conducted [20] predict that the nanodisks realign to match crystal structures at the boundaries, making the nanobeam

a single-crystalline. As explained in Chapter 1, polycrystalline materials have higher resistivities as a result of grain boundary scattering of conduction electrons [22]. Electrical characterization of these nanobeams then, can inform one of the details of the structure of the nanobeams themselves. To this end we embark on a project of electrical characterization of these nanobeams using the methodology invented in Chapter 2.

3.2 Characterization

Not all of the nanoplates inside the solution join into nanobeams so the end-solution contains individual nanoplates, very small nanobeams, and medium and large nanobeams. The contents of the solution thus make centrifugation difficult since it is filled with particles with the same makeup and consistency.

Figure 3.1 shows images of the nanobeam solution with different perspectives. In higher magnification images one sees that the beams are by no means uniform or smooth. These nanobeams are made of triangular and hexagonal constituents and the directionality of the joining of new silver plates to the edges is not predetermined. The typical nanobeam height is ∼200 nm and width is ∼700 nm, with an average length of 40 μm. If enough plates join in such a manner that a separate direction of growth is initiated, branches appear along the nanowire axis, as seen in Figure 3.1b. There are often intertwining branches and large changes in wire diameter as one follows along the wire axis. The AFM has been employed to confirm that the nanowires are largely flat on top and have a rectangular cross section.

Figure 3.1 (a) and (b) also portray the typical makeup of the beam solution. Due to continual plate joining this type of nanobeam has a high probability of conglomeration where otherwise separate particles join to make large clusters.

3.3 Electrode contacts

In order to electrically and hence structurally characterize the nanobeams one must first initiate electrical contact. Figure 3.2 shows gold contacts deposited on nanobeams prepared for a 4 point probe measurement. The principles of 4-point-probe measurements are discussed in Chapter 1 and the method of electrode fabrication is discussed in Chapter 2. For the purposes of measuring the resistivity of the nanowires it is important to note that the fingers are 3-4 μm apart and 2-3 μm thick.

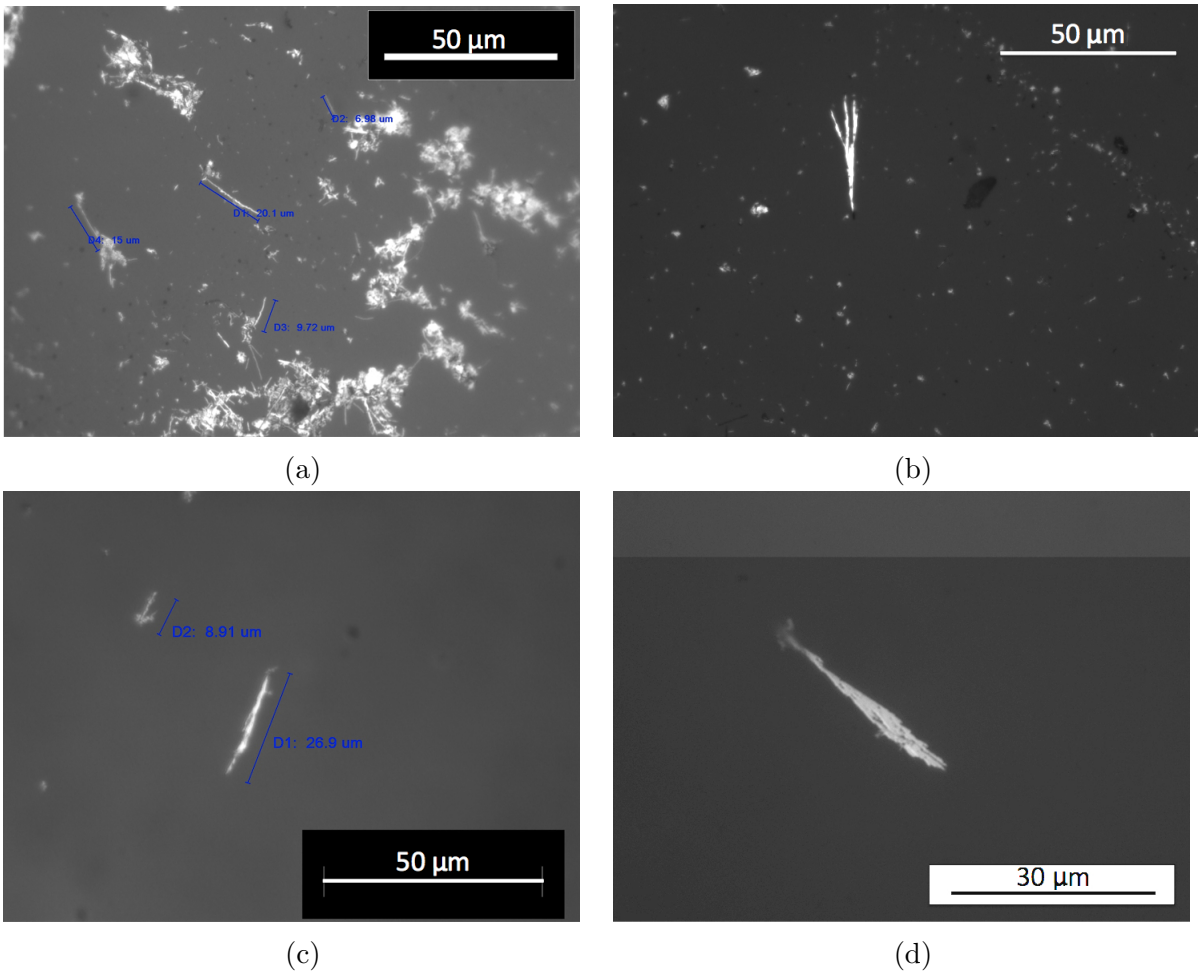

(a) (b)

(c) (d)

Figure 3.1: Various optical microscope images of nanobeams. Images (a) and (b) show the nanobeams at lower and higher magnification before centrifugation and (c) and (d) show individual nanobeams afterwards. Almost all nanobeams have branches of various sizes and in (d) the nanobeam branches join back into the main nanobeam axis

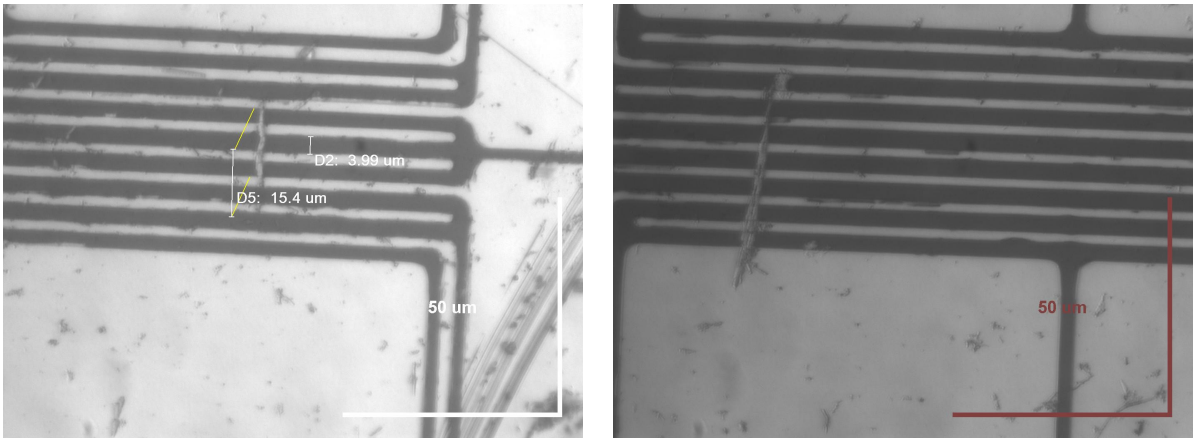

(a) (b)

Figure 3.2: Optical microscope images of gold electrodes deposited on top of the silver nanobeams to allow for a four point connection

3.4 Probe results

Some of the gold electrode connections to the silver nanobeams were initially poor, with non-linear resistances appearing. Although it wasn't immediately realized, it was later confirmed that this is due to an intermediate insulating layer that separates the beam from the electrodes. The modeling of this layer and the procedure designed to tackle this problem is explained in depth in Chapter 4. Instead, several nanobeams were found that did have adequate connection, and these were the nanobeams tested. Figure 3.3 shows the I-V curve collected from one such beam.

The measurement was taken using a current ramp sweep as the driving power source on probe 4. V4 is then the voltage measured on that probe representing the entire 2-probe response of the system. In order to extract the true resistance of the nanowire the contact resistance has to be removed from the equation, and so the two middle probes measuring the voltage are employed. By subtracting the voltage between these two probes on can extract the difference in voltage caused by a known current in the nanobeam portion between the two electrodes, leading to the sole resistance of 0.37 Ω in this case. SEM and AFM size measurements put the width at the thinnest region to be 1.4 μm, the length between the two middle electrodes at 3.65 μm, and the height at 194 nm. Using these dimensional values one can calculate the resistivity of this nanobeam to be 2.7x10^{-8}Ω·m. Bulk silver resistivity is 1.6x10^{-8}Ω·m.

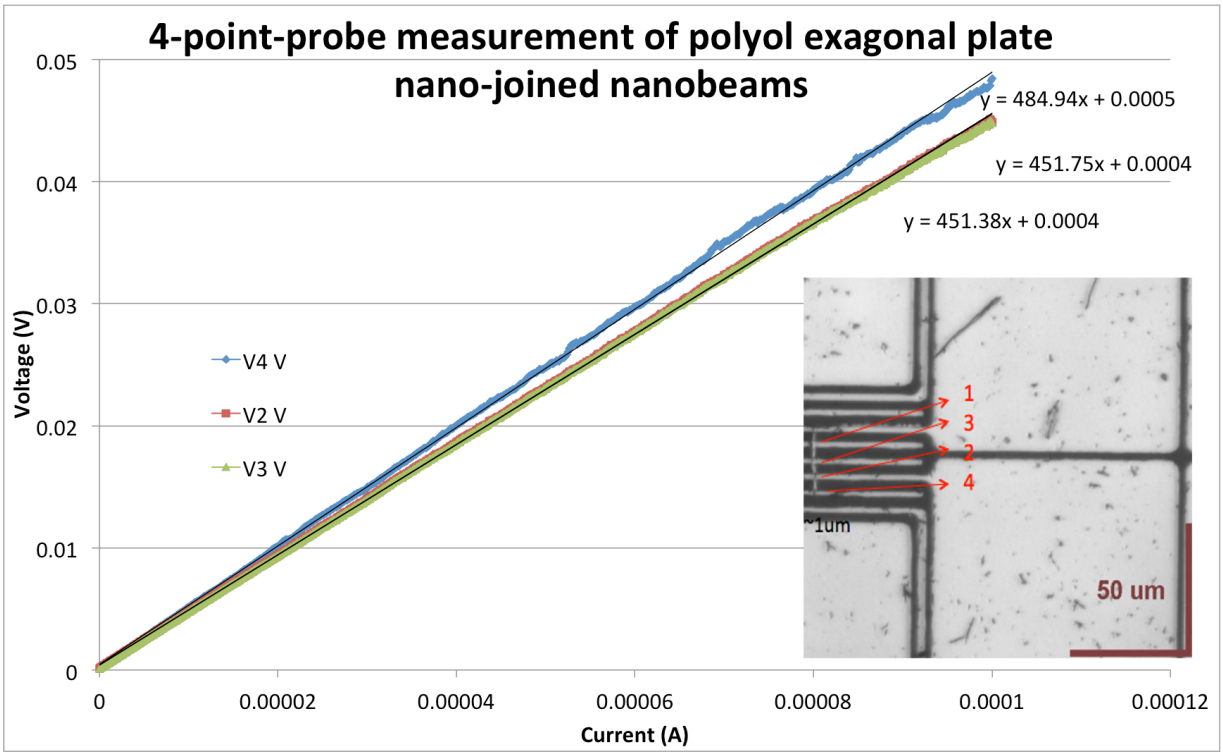

Figure 3.3: A 4-point-probe measurement of a nanobeam trapped under 4 electrodes. V4 represents the voltage measured from the current driving probe, while V2 and V3 are measured from the two middle probes, all with respect to V1 (common). The resistance of the wire between the two middle probes is measured to be 0.37 Ω.

Four other Nanobeams were tested and were found to have resistivities in the order of $10^{-6}\Omega\cdot$m-$10^{-8}\Omega\cdot$m.

3.5 Analysis

The very low resistivity of this type of nanobeam is affirmation of what physical models have already shown [20]. Using computer models it has been predicted that the crystal lattices of the constituent nanodisks line up to form a single crystal nanobeam. The nanobeams seem to operate as crystalline structures with the beam resistivity falling within an order of magnitude of the bulk material. Other papers such as [73, 25, 32, 74] show that crystalline silver nanostructures generally retain the very high electrical conductivity of bulk silver.

The resistivities calculated in these papers match the results calculated in the previous section.

The mechanism by which silver plates join together and align lattices to create crystalline material is discussed elsewhere [20] and is beyond the scope of this thesis. However our experiment confirms that one can assess electrical properties of small objects using the electrical contact patterning procedure describe in Chapter 2 and a probe station.

The great variance in resistivity measurements calculated, point to several sources of error present in the measurements. The first source of error is in the failure of the nanowire structures before accurate SEM and AFM measurements were taken. The sources of this structural failure are discussed in Section 3.6. Due to the structural failures appearing in the time between electrical characterization and microscopy (Figure 3.4), it wasn't possible to measure exact values for the dimensions of the nanobeams. Furthermore, the AFM measurements were noisy and showed very large roughness measurements for all surfaces making it difficult to ascertain exact height differences. For these reasons the resistivity measurement is estimated to be accurate within an order of magnitude, which results in a deviation of resistivity measurements calculated.

3.6 Nanobeam endurance

One interesting side effect of the nanobeam confinement under the electrode fingers is the testing of the durability of the nanobeams. Several months after the measurements were done, SEM imaging of the nanobeams were performed and almost all the samples were missing in part. Figure 3.4 shows SEM images of these nanowires 5 months after the initial fabrication.

Due to the non-uniform and violent nature of the damage to the nanobeams it is likely that the cause is not a minor process, rather it is likely that major changes are created in the structure over time. Elechiguerra and coworkers [75] showed that after several months in air, silver nanostructures show massive deformities indicating corrosion and silver sulfide formation. This weakening of the crystal structure, coupled with vibrations from the surrounding substrate, in particular when handling or experimenting on the substrate, may split the nanobeams to pieces, which can then dissociate from the surface over time.

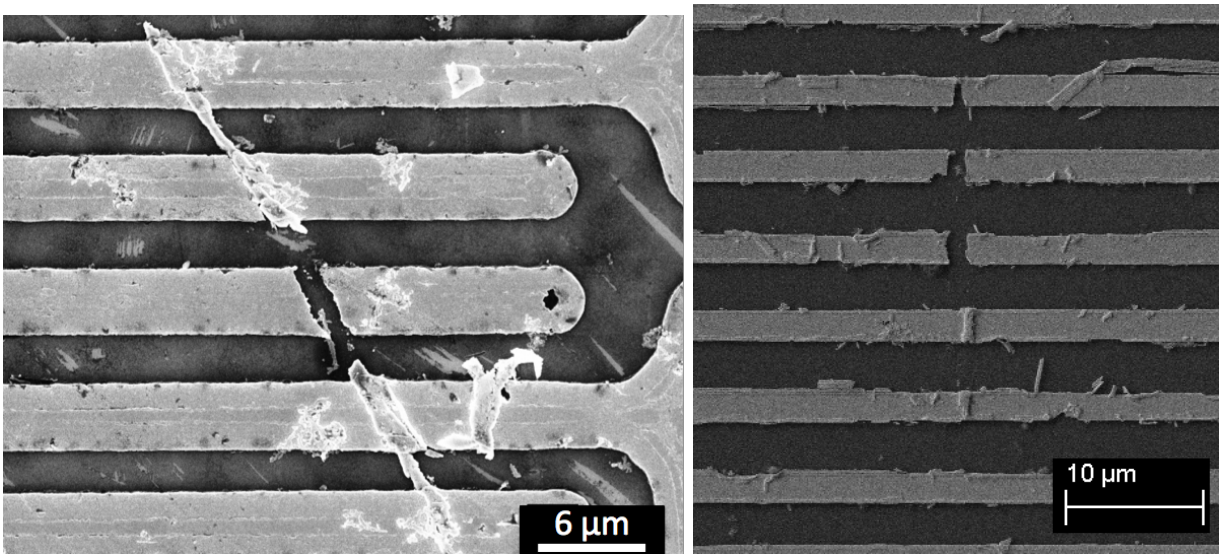

Figure 3.4: SEM images of two of the tested nanobeams taken five months after fabrication. Parts of the nanowire have been completely severed with the gold on top also sometimes missing.

3.7 Limitations

Although the process outlined in this chapter is novel and at the state of the art, it nonetheless has limitations.

The first limitation is on the theoretical assumptions of the 4-point-probe measurement as applied to these nanobeams. These nanobeams often have small non-uniformities, which defies a requirement for the electric field being constant in between the two outer probes. Non-uniformities also mean that resistance measurements for the individual parts between the electrodes can no longer be compared, since the resistance changes significantly depending on the cross section of the nanobeam.

The second limitation is regarding resistivity measurements of objects with very small cross sections. It has been shown that nanobeam resistivity changes with diameter. This means that the resistivity calculated for this type of nanowire may not be completely accurate since depending on the diameter of the nanobeam, slight changes can occur in resistivity.

Both of these limitations have minimal impact on resistivity measurements, and provide for divergence of less than an order of magnitude from the resistivity measured.

Chapter 4

Welding of nanowires using current-induced Joule-heating

In order to create complex devices out of a collection of nanostructures, one needs to be able to initiate reliable physical contact between the constituents. Important group functions such as conducting electricity, transporting plasmons, mechanical movements, and electrochemical junction creation are all made possible by welding the two or more pieces together. So it is not surprising that welding of silver nanowires, which have been used individually for all of the above, has been experimented with for a decade. For the purposes of this thesis the nanowire-nanowire contact region will be referred to as a "junction" or a "joint".

The nanowires used for the welding experiments in this chapter were synthesized using the polyol method, described in detail in Section 1.1.2. The relevance of this project is enhanced by the fact that this type of nanowire is very easy and cheap to fabricate en masse, and have never been welded together before. These nanowires have great features such as very high aspect ratios (up to a 1000), low resistance, and smooth surfaces, making them ideal for many applications such as plasmon resonance and electron transport. The tightly packed optimal mask design allows for the possibility of up to a 100 useable nanowire-nanowire junctions per cm^2 of substrate. Furthermore photolithography and electrical probing are simple and common procedures. The economics and the speed by which nanowires can be accessed and welded together makes this project of great importance to possible industrial expansion.

Despite previous attempts to initiate reliable welds between nanowires, as discussed in detail in Chapter 1, there has not been a satisfactory discussion of the feasibility of nanowire

welding at an industrial scale required for sensor or integrated circuit fabrication. Details such as intermediate layers and the mechanism for weld generation are often left out of research papers released on nanowire welding. Although electrical access to nanowires have been made possible using photolithography in the past, the welding of nanowires has never been tried in mass scale with the simple and economical procedure outlined in Chapter 2. In this chapter, pads fabricated using photolithography will be used to electrically weld silver nanowire junctions until a reliable ohmic contact is achieved. An ordered procedure for the application of current and voltage to the junctions will be invented to make the welding procedure more automatic. An intermediate layer will be identified and it will be shown that the electrical recipe invented will break down the layer sufficiently for an ohmic connection to exist.

4.1 Setup

The nanowires are drop-cast on the surface of SiO_2 substrate chips, dried, and the PVP is cleansed by washing with acetone and IPA. The type of electrode chosen for patterning on top of the nanowires was the pad array, seen in Figure 2.3, with spacing between the pads set at 4 μm. 4 μm was chosen by considering that the nanowires used are on average 10-15 μm long. Nanowire alignment is random and so will likely have an angle with respect to the pad edges and a certain portion of the nanowire will ideally be buried under the pad for better contact. Added to the fact that due to overexposure the trenches often end up larger than designed on the mask, it is easy to see that this distance is the ideal choice. An example of the finished pad and nanowire product is shown in Figure 4.1.

The welding of the nanowires is initiated using the two probe setup on a probe station. One probe is taken as source and the other as ground with the response recorded on the same probes. The square gold pads' end-product has an edge length of about 99 μm with the trenches ~ 4 μm wide.

4.2 Distinguising two types of junctions

In welding large numbers of nanowires, two separate types of junctions have been identified. The reason for the distinction is the different levels of voltage required in the initial steps, success rates, and the mechanism by which each type initiates the weld.

The first type will be called the overlap junction. As the name suggests, these are junctions that are already likely in contact due to a shared region of overlap between the

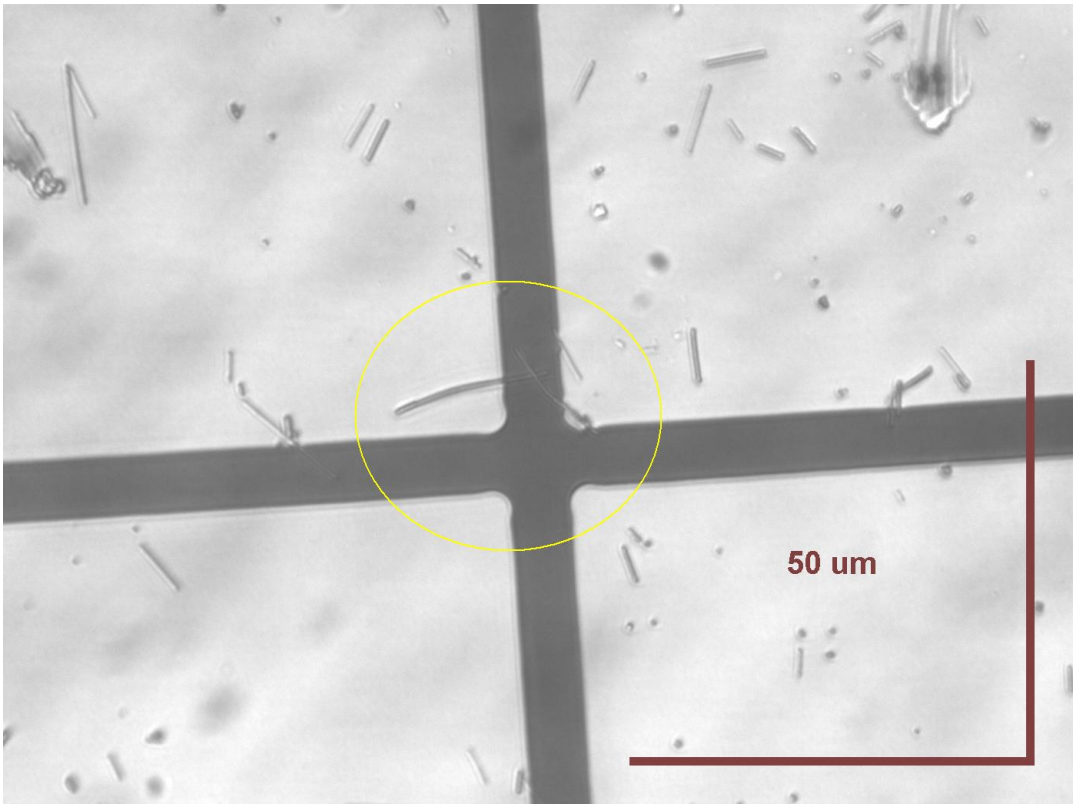

Figure 4.1: Finished electrode-nanowire device setup. The nanowires circled are overlapped and are a possible candidate for the welding experiment to follow. This image was taken using an optical microscope.

two wires. An example of an overlap junction situated between two gold pads ready for welding is shown in Figure 4.2a. The main distinguishing feature of this type of joint is that molten regions have to travel downwards to join the structure required to complete the weld.

The second type of junction welded will be called the gap junction. The gap junction as the name suggests represents the junction between two nanowires that has a small separation at the closest point. If this separation is small enough, we found we were able to achieve an ohmic connection using electrical current. An example of a gap junction is illustrated in Figure 4.2b. The main distinguishing feature of this type of joint is that molten regions have to travel horizontally to join the structure required to complete the weld.

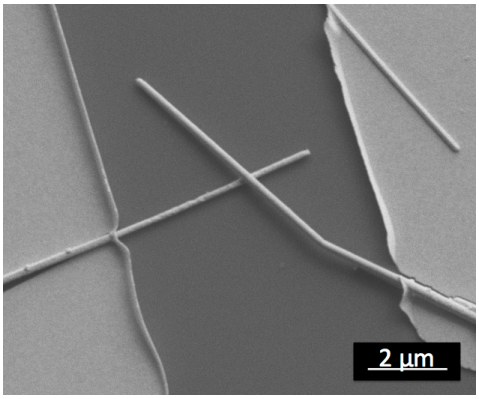

(a) Overlap junction

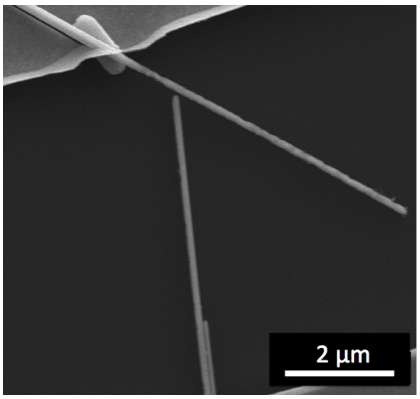

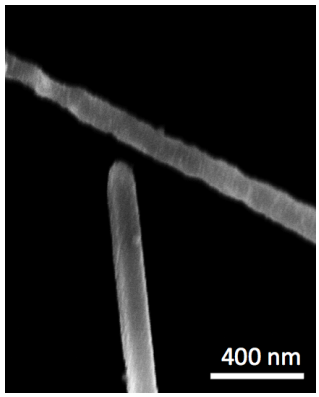

(b) Gap junction with low (left) and high (right) magnification. This particular gap spans approximately 73 nm at the smallest point.

Figure 4.2: Examples of the two types of junctions discovered

4.3 Overlap junction

As experimentation welding the wires began it soon became clear that an ohmic connection was not immediately possible, even with a single nanowire spanning two electrodes. Measurements conducted on single nanowires showed the resistance between the two pads to be on the order of 1 TΩ which is much larger than anything at these physical dimensions. Upon pressing the voltage further a sudden surge of current appeared, signaling a rapid reduction in contact resistance.

4.3.1 Intermediate layer

Modeling

This type of rectifying response was immediately identified to belong to a diode-like structure. In effect, if there happens to be a non-conductive layer between the nanowire and the gold pad, it will create the conditions for such a response to occur. The junction between a metal and a dielectric is called a Schottky diode. The metal-dielectric-metal junction on the other hand, would create two diodes facing each other, each with its own forward and breakdown voltages. Due to the fact that gold is largely inert [72] and is evaporated on top of the wires, it is unlikely that the dielectric layer originates from it. The insulating layer likely comes from the nanowires, and so the layer will also exist between the two silver

nanowires being welded together. This is consistent with the observation of a significantly larger break down voltage with junctions as opposed to single nanowires traversing between two pads. The idealized circuit model for the entire system would then look something like the schematic presented in Figure 4.3.

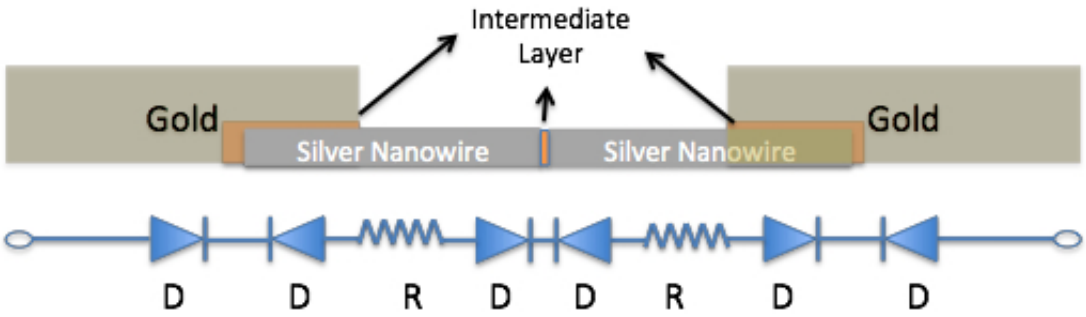

Figure 4.3: The created representation of the nanowire-pad system is shown with the idealized circuit schematic below. In order to conduct significant current through this circuit, one would have to meet all the forward voltage and breakdown voltage criteria of the diodes added together.

Using the circuit diagram it is clear that no substantial current will flow through the circuit until the voltage condition of all the diodes is met. This means that the forward biased diodes will have to reach a large enough forward voltage, and the reverse biased diodes will have to reach breakdown region. Since the condition for all diodes must be met in order for current to flow, the voltage applied to the entire circuit must be above the added voltage conditions of all the individual devices.

Intermediate layers are then very important to the welding process of polyol metal nanowires in industry, since despite the setup, there will likely be a layer of non-conducting substance between two wires. Among the many reasons for this is that the nanowires are fabricated in a separate solution with a polymer surfactant, making surface contamination in solution and during transfer inevitable. Furthermore, once the nanowires are deposited, they are prone to corrosion in air. For the overlapped junctions, the intermediate layer will likely be of the same nature as the gold-silver contact. For gap junctions, however, it will likely be a combination of the contamination layer and the space between the two nanowires. In order to weld metal nanowires one will have to find a way to surpass this layer.

As for the identity of the insulation layer, there are several candidates. The layer could consist of a corrosion or a sulfide layer on the surface of silver as these nanowires are prone

to such layer growth [75]. The layer could also be a silver oxide layer or consist of left over PVP signaling that the cleansing attempts were insufficient at removing the polymer. It is also possible that there is a layer of photoresist remaining on the nanowires from the pad fabrication procedure. The photoresist is removed from the nanowires during the developing step of the photolithography patterning, and it is possible that residual layers remain, cutting off the gold from the nanowires beneath. The latter is unlikely, since it does not explain why as the time between fabrication and welding increased, the power required to break down the intermediate layer was also raised.

Removal

A procedure is designed to remove the intermediate layers or at least mitigate their effects, using Joule-heating. To solicit a current response one will have to ensure that a current pathway exists between the metal nanowires. An ohmic connection will be a signal that the weld is complete. A well-known method of destroying diodes is to surpass their breakdown voltage by a significant amount. This concept will be employed to destroy intermediate layers, weld the nanowires, and thus achieve an ohmic connection. The procedure goes as follows:

1. For thinner nanowires that melt with lower power expenditure, it is advised that incrementally larger constant voltages, applied to the two electrodes, be used to find the initial surge voltage. This is the voltage at which the current response first spikes, indicating breakdown of the dielectric between the metals. The power dissipated from a linear circuit element under a constant voltage is $P = \frac{V_o^2}{R}$, which is inversely proportional to the resistance of the element. While the resistance is very high at the outset, the power will remain in a safe range. Power levels in response to driving currents are represented by $P = I^2R$, which being directly proportional to resistance will more often burn the nanowire before a weld is initiated, as confirmed in experiment. The inverse relationship to resistance also means any reduction in resistance will cause power spikes and a current limit dependent on the voltage level must be imposed. By experience, current limits of 50-500 pA are generally safe up until 10 V.

2. The above step can be replaced with a voltage ramp sweep for resilient nanowires with fast heat dissipation. By keeping the ramp moderately slow and the current limit low, one can increase the ramp maximum in search of the surge voltage. Once the surge voltage is found, a measurement with a ramp maximum just above the surge

voltage must be repeated. As the dielectric breaks down upon repeated measurements, the surge voltage will decrease. Once the surge voltage reaches a minimum, the current limit can be increased, further decreasing surge voltage upon repeating similar measurements. Once the surge voltage reaches a safe range (*i.e.* <1 V) the next step can be initiated. Step #2 is required to decrease the initial resistance so that a current ramp will not immediately result in the destruction of the nanowire

3. A switch to forcing current ramps occurs once the above step is complete. The power response to ramp currents is $P = I^2R = n^2I_{step}^2R = n^2CR$, with n being the number of steps and C as some constant. The linear dependence on resistance means that as the nanowires weld and resistance drops, the power also drops, leading to a self-executing process. It is prudent to set the voltage limit and the sweep maximum to no more than twice the final values in the previous step. Multiple current sweeps must be completed with increasing ramp maximums until an ohmic contact is established, signalled by a linear voltage response. An ohmic signal means that the nanowires are now welded, with an ohmic connection, however it does not mean the lowest resistance possible has been reached. There is no method of knowing the lowest resistance achieveable but experience, through driving junctions to failure.

4. For nanowires that melt with lower power requirements, a constant current source with measurement time ranging from 50-500 s can be utilized. The power response of a constant current signal is $P = IV = I_o^2R$. The constant current also benefits from the self-executing nature of direct dependence on resistance, with a lower risk than the current ramp, due to the n^2 term not being present. However the process of incrementally increasing constant current measurements is much more time consuming than simply employing the current ramp. An ohmic connection is established in this case with a flat voltage response, that is linear with a slope of zero.

The above recipe can be used with one probe as the forcing source and the other as the common. For some cases applying the process in both directions might help with the welding due to the directionality of the Shottky diodes. Figure 4.4a shows the current response of a freshly tested sample junction to a voltage sweep (step 2). The surge voltage, once found, was decreased by repeating the same measurement with incrementally increasing maximum currents. After the final sweep, where the surge voltage reached 0.8 V, the switch to current sweep was initiated. The response to the current sweeps (step 3) is shown in Figure 4.4b. In this plot, the first two sweeps represent the current ramps used to attempt the welding of the wires, although there were many more current ramps conducted in between the ones shown. The last sweep is represented by the small ohmic green line, measuring a resistance of 2154 Ω for the entire junction-pad system.

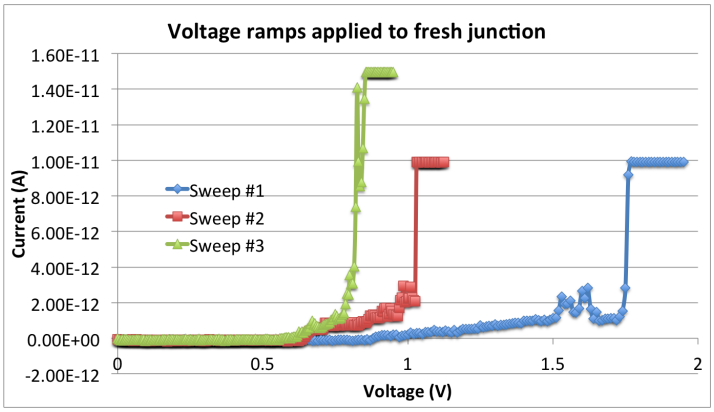

(a) Voltage response of an overlapping junction under a voltage sweep. The current maximum for the first two sweeps is 10 pA and 15pA for the third.

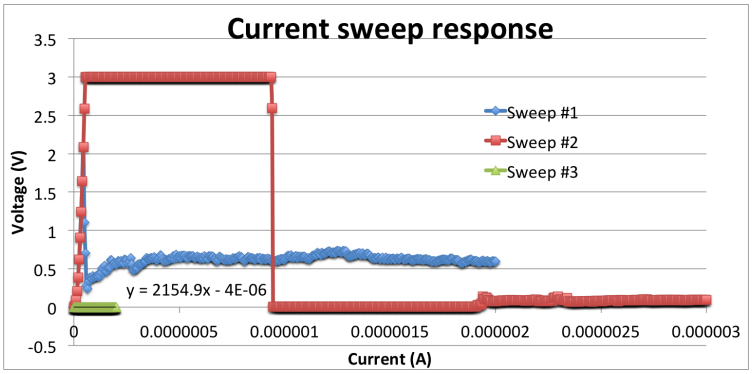

(b) Current sweeps are used to completely breakdown the dielectric leading to a reliable weld. Sweeps #1 and #2 represent two of the intermediate current sweeps performed on the nanowires, although there is many more measurements in between.

Figure 4.4: I-V curves of the steps required in welding nanowires together as explained in Section 4.3.1

4.3.2 Welding results

Several overlapped junctions were successfully welded. Two examples of this type of welding and the final resistance achieved are displayed in Figure 4.5. The effects of the weld are nearly identical in both junctions. The heat caused by the resistive heating at the junction contact caused the top nanowire to melt at the tip. The ohmic nature of the system signals that the weld is indeed complete. Several minutes after the weld they were still ohmic with the same resistance. Measurements conducted a day after the final welding, show that

most of the devices no longer have the same resistances.

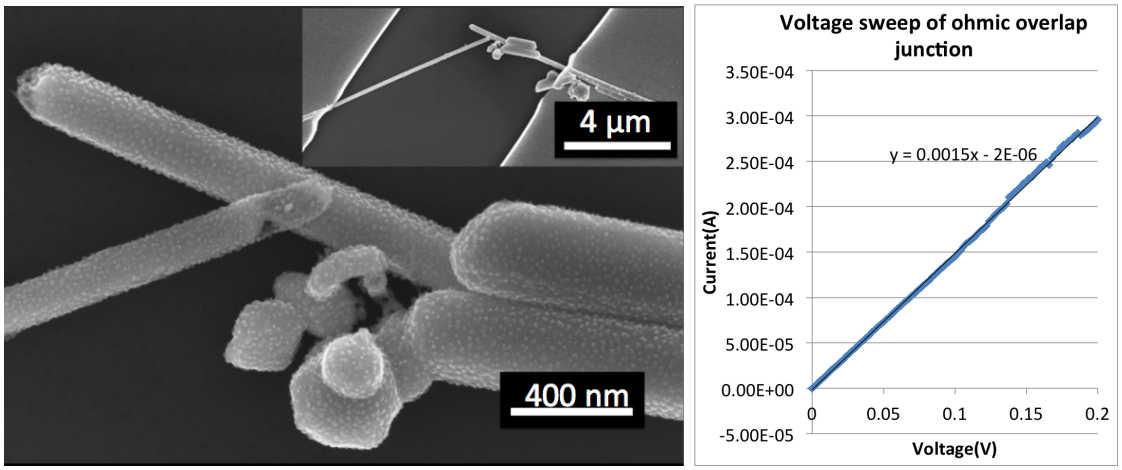

(a)

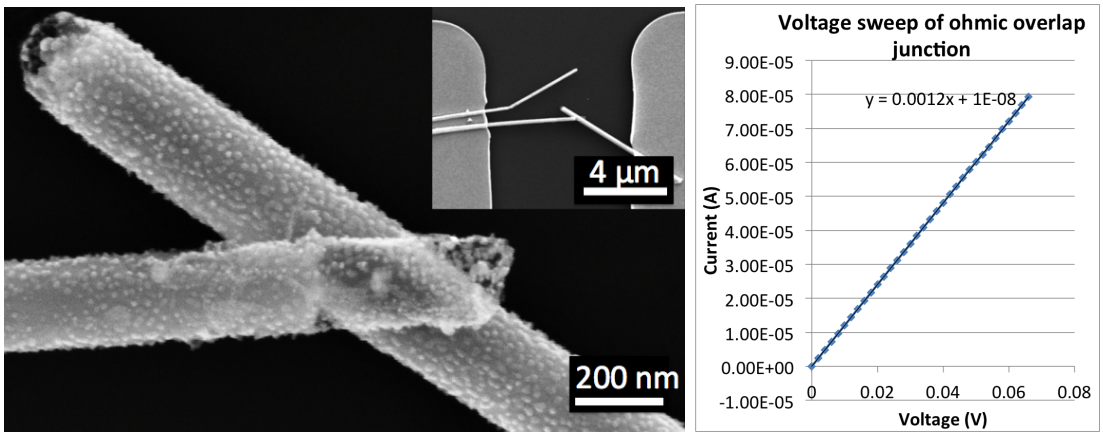

(b)

Figure 4.5: Two examples of overlapped nanowires welded together using the electrical procedure. The resistance of the entire device shown in (a) comes to 666 Ω and 833 Ω for (b).

Although the resistance of the system is known, it is difficult to measure the resistance of the junction specifically. The nanowires possess different diameters and contact resistance is not properly accounted for in a 2-point-probe measurement. It is suspected (tested in detail in Chapter 5) that the nanowire-gold contact resistance has been reduced significantly by this point, however it is not guaranteed that it is completely gone. For the same reasons the resistivity of the system cannot be calculated.

4.4 Gap junction

4.4.1 Intermediate layer

Surprisingly the gap junction behaves in the same manner as the overlap junction in response to initial voltage sweeps. The possible reasons for this will be discussed in detail in Section 4.5, however one can hypothesize that the space in the gap acts as an extension of the dielectric, and has to be broken down for electron tunneling to occur. For this reason the same procedure described in Section 4.3.1 is deemed appropriate for welding this type of junction.

4.4.2 Welding results

An example of one of the many such junctions tested is shown in Figure 4.6. Since conducting across space requires substantially more energy given to the electrons that would otherwise tunnel through a thin layer of dielectric, the heat generated as a result is also substantially larger. As seen in the Figure 4.6b this extra heat can cause the nanowire tips to completely melt near the contact.

Very few gap junctions survived the extreme heat transferred to the system during current conductance. There seems to be a limit to the gap distance and the diameter of the nanowires for gap junction welding to occur, likely due to the fact that enough silver has to be available to traverse the gap.

4.5 Analysis

Using a three-dimensional finite-element modeling program, Tohmyoh [18] showed that the temperature profile of a single silver column under current consists of a peak in the center of the two ends. Furthermore, there is a spike in heat generation at the contacts or at grain boundaries, because of the high local resistances at these points. The generated heat is proportional to nanowire diameter in the region and the current passing through it. Tohmyoh also showed that there is an energy band where below the band the energy is insufficient for joining and above it the wire burns due to excess heat.

This analysis is imperative to understanding the dynamics of welding within metallic nanowires, our nanowires included. This will be used to explain several changes in the nanowires during the welding process in the following sections.

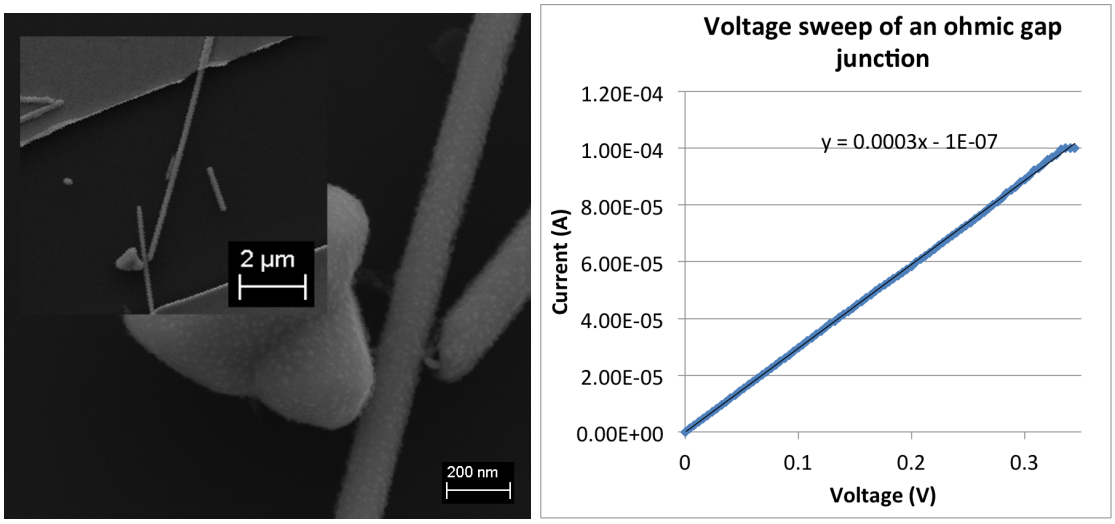

(a) The image of a gap junction in the inset and the final ohmic result on the right. The silver nanowire junction is welded until a resistance of 3333 Ω is reached, representing the overall device resistance.

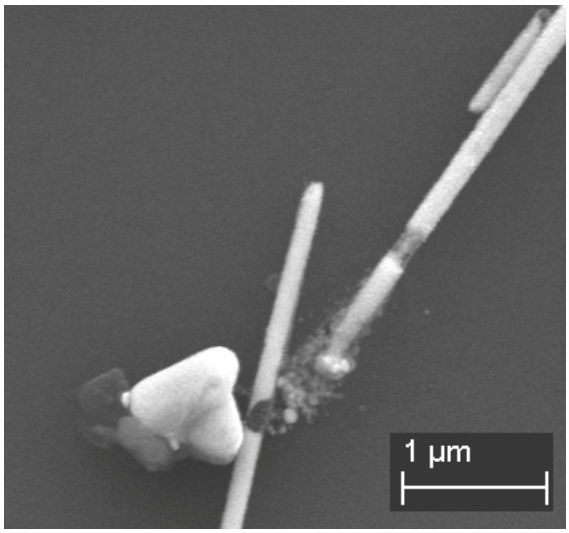

(b) The high heat created from the welding procedure applied to a gap completely destroyed the tip of one nanowire and the side of the other. The nanowire bodies away from the cyontact remained intact.

Figure 4.6: The welding of a gap junction and the result

4.5.1 Change in form

Overlapped junctions

The nanowires shown in Figures 4.5 are very good examples in illustrating the change in form one can expect from Joule-heat welding of overlapped junctions. According to Tohmyoh the majority of the heat generated will be at the contacts and in the middle of contacts along the nanowire axis. This means that, supposing Joule-heating is the only major effect on the nanowires, most of the structural changes will occur in these locations. Looking at the figure it is clear that the bodies of the two nanowires away from the contacts are intact. At the contact however, the top nanowire has descended from the heat generated in the contact and has been welded to the bottom nanowire.

Gap junctions

Recalling that current will only flow if all the voltage requirements for the individual parts are added up, one can qualitatively analyze the gap junction welding phenomena. The voltage required for discharge across gaps in bulk materials is governed by Paschen's law. Briefly, Paschen's law states that in small gaps, if the pressure is kept constant, as the gap gets smaller, the voltage required for discharge increases. In gaps smaller than 5 μm however, Paschen's law no longer applies fully and another phenomena called ion-assisted field emission dominates [**?**]. Basically, the ions created at the surface of the cathode due to quantum mechanical effects enhance the electrical field, causing instabilities that lead to early breakdown of the particles in the gap. The relationship between breakdown voltage and gap distance changes to reduce as the gap gets smaller, within this range.

The discharge voltage added with the intermediate layer requirements sum up to a breakdown voltage larger than those seen in overlap junctions. Since the only form of energy dissipation at this scale occurs through photons and phonons, with phonons dominating to a large extent, this means that the heat generated is also larger compared to nanowires already in contact. The extra heat can then damage the nanowires and this is seen in all the gap junction nanowires tested, including the one in Figure 4.6.

The greater heat in gap junctions can be both a blessing and a curse. Due to the existence of the gap, a greater amount of heat is required to sufficiently melt the nanowire for connection to occur. If the heat generated however is too high, it can cause massive structural changes to the nanowire. In order to confirm whether Joule-heating is responsible for gap welding and to further examine the possibility of such weld, the following experiment is constructed.

A single nanowire attached to a gold pad on one side and separated from another pad with a small gap (400nm) is located. The nanowire is chosen with a reservoir of silver at the tip. The procedure explained in Section 4.3.1 is the used to weld the silver reservoir tip to the respective pad, across the gap. The setup is shown in Figure 4.7 with the before and after picture side by side.

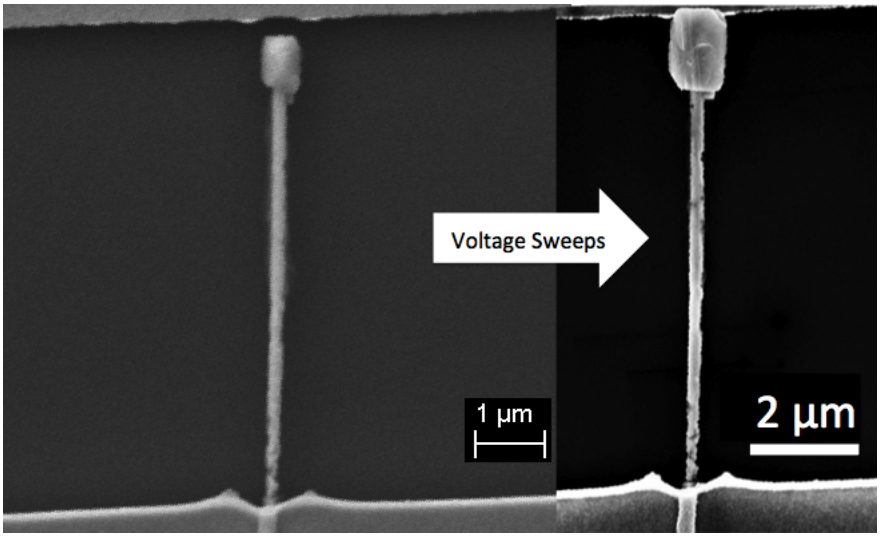

Figure 4.7: A single nanowire spanning two pads is found with a silver reservoir at the tip closest to the gap. Voltage sweeps (as in step 2 in Section 4.3.1) are conducted across the two pads. Electric current is observed and the reservoir expands from 750 nm to 1.2 μm to close the gap.

By close inspection of the before and after picture, an explanation of the welding phenomena can be constructed. Using the deformities in the wire, one can measure the distance between parts of the wire and the pads before and after the sweeps are completed, to account for any movement. After measurements it becomes clear that the nanowire itself has not moved in relation with the pads. This means that physical stretching and any other phenomena that involve the entire structure are not responsible for the movement. When measuring the reservoir surface area however it immediately becomes clear that the reservoir has substantially increased in length, going from 750 nm to 1.2 μm. The discrepancy is almost exactly the length of the gap. This means that all movement originates from the part of the structure closest to the gap and the rest of the structure is left largely undisturbed. Our results indicate that in fact local area melting, resulting from Joule-heating caused by electron transfer presumably through tunneling, is responsible for junction gap welding. Furthermore, this proves that gap junction welding is possible if

only the constituents have a large enough supply of metal to bridge the gap. Otherwise the massive heating will simply destroy the structures as seen in Figure 4.6b.

4.5.2 Welding threshold

Taking a queue from Tohmyoh [18], the nanowire junctions are modeled as cylindrical tubes of metal connected at a point. Tohmyoh, using an invented welding parameter, modeled this situation and showed that there is an energy region where the heat produced in the contacts is high enough to initiate welding without the heat in the center of the nanowires reaching the level of splitting the wire in half. Our experimentation largely confirms this with a few exceptions. Our polyol nanowires had a variety of diameters, and due to their higher resistivity, thinner nanowires have smaller threshold energy regions, making junctions with a thin wire much harder to weld.

With gap junctions however, as discussed above, the heat generated by the tunneling is much higher, so that the parts closest to the gap region will most likely melt first. Indeed no gap junctions have yet been tested where the nanowire center melted before the contact.

4.5.3 Reliability

The welds generated by this process were tested over time to measure the reliability of the welds. All the experiments discussed above were tested for how long the ohmic connections would last and all passed 5 minutes. Several of the welded joints were tested on the order of days, however, and few survived without a major increase in resistivity.

There are a few hypotheses for why this is. Khaligh and Goldthorpe [77] showed that polyol silver nanowires arranged in a mesh corrode but much faster in higher temperatures than standard lab conditions [75]. It is likely that the temperature increase resulting from the welding procedure causes a spike in corrosion speed, causing an increase in the resistivity of the entire system.

The second reason why the resistivity could increase over days is that the nanowires weld together under stress, and there's a constant pressure to separate. Coupled with the fact that the welding region of Joule-heating welded nanowires is often very thin [19], it is possible that the weld cracks and separates over time.

4.5.4 Failure

The failure mechanism of the nanowires is investigated and is found to largely confirm Tohmyoh's [18] analysis. The majority of the damage occurs at the contacts with occasional failure at the center of the nanowires between two contacts. The nanowires shown before confirm this, but also the SEM image of a model example where extreme currents were forced between the two pads for prolonged periods is shown in Figure 4.8. In this figure the burn regions are circled for clarity. Nearly all the failed nanowires observed illustrate the same pattern, with each nanowire going through hours of current conductance. These results rule out other proposed sources of silver nanowire failure such as electromigration.

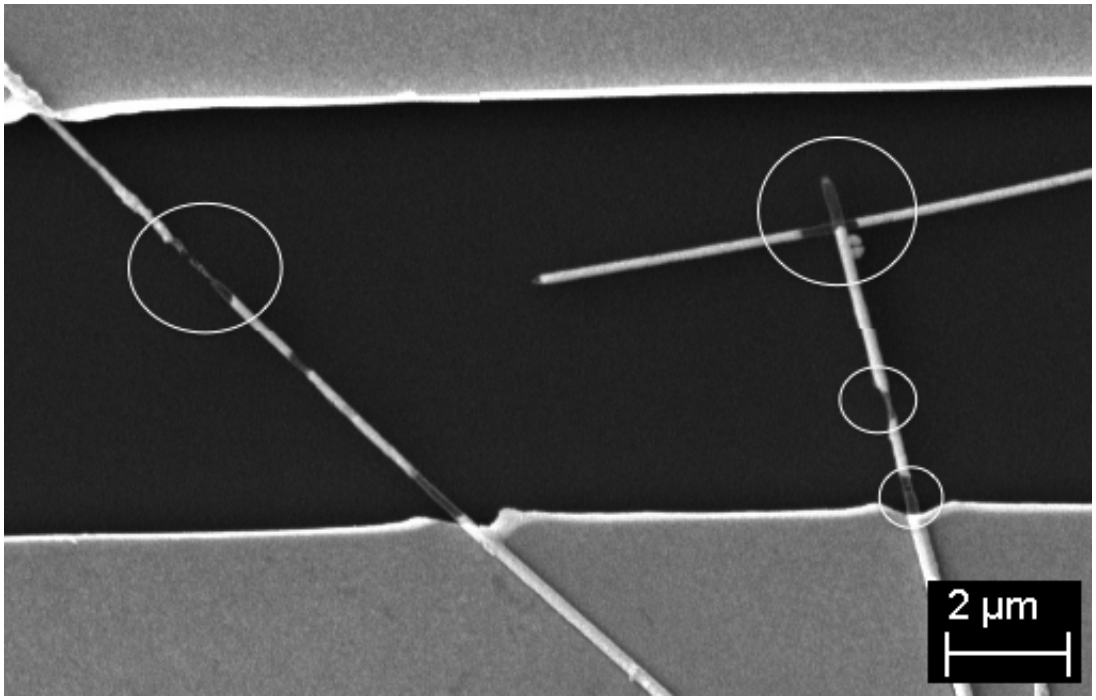

Figure 4.8: A model example of Tohmyoh's explanation of the heat pattern and hence failure in silver nanowires. Extreme currents were forced between the two pads and through the nanowires for prolonged periods of time. The burns are generally located at the contacts or in the middle of the nanowire between two contacts.

4.6 Limitations

There are a couple of limitations on the analysis put forth that are worth mentioning. The first is that the critical analysis of the joint region subsequent to the welding process was not performed due to a lack of proper equipment. The overlap junctions in particular showed a hollowing of top nanowire near the tip that would be very interesting to investigate. It is possible that this this change of structure could make the welding process ineffective and further study is necessary.

Another limitation is the formation of surface corrosion on the nanowire surfaces as a result of heating the wires. Corrosion can have significant impact on the device performance and minimizing surface layers would be of interest. If the welding process changes the nature of the welded nanowires, it could pose serious concern regarding this type of nanowelding as the method of choice.

Chapter 5

Contact resistance reduction using Joule-heating

Perhaps the greatest impediment to the new age of even smaller electronics is contact formation. Due to the very small scale of the objects and the contacts used, contact resistance begins to play a major role in device energy efficiency, resistive heat generated and noise introduced into the system [23]. As explained in Chapter 1, a common method of by-passing contact resistance for a resistivity measurement is using a 4-point-probe apparatus [69]. The problem, however, is that in structures that are not long enough for four electrodes/probes to cover them, this method is impossible or otherwise expensive. Furthermore, the 4-point-probe technique is used only for measurements and not for functions such as efficiently conducting electricity. Bid and coworkers [78] used a different method of establishing a contact, specifically by using Pb-Sn solder, to reduce contact resistance. Others simply reduced the temperature of the sample to below 4 K to reduce contact resistance [37, 79]. In another case, a regression was created based on a formula, estimating contact resistance to remove it from the equation [70].

Equipment that can take temperatures below 4 K are very expensive, especially as the price of helium goes up. Using solder or other mechanism of strengthening contacts can introduce contamination, and be very difficult and time consuming, especially for nanowires that are short enough to render 4-point probe measurements impossible. To solve this problem, we have embarked on a project to reduce the contact resistance between metallic structures using Joule-heating. Joule-heating can be applied directly to the contact and does not require special equipment. In particular, a nanowire-pad arrangement is created using optical lithography and the common lift-off process. By probing the pad with a

semiconductor analyzer the contact resistance between the nanowire and the pad was greatly reduced.

Another problem with contacts that appears as dimensions get smaller is rectifying behavior due to contamination playing a larger factor. Great diligence and expense is incurred in keeping systems free of contaminants and maintaining high vacuum in order to create ohmic contacts [24]. An electrical recipe to lower resistances between two metals was explained in detail in Chapter 4 and was used to remove intermediate layers that exhibited rectifying properties. Using that same method, the Schottky contacts between silver nanowires and gold pads will be broken down.

5.1 Experimental setup

The nanowires used in this experiment were purchased from Blue Nano Inc. These silver nanowires have pentagonal cross sections and are made using a variation of the polyol process, explained in Chapter 1. The average diameter of the wires was 90 nm with the average length approaching 40 μm.

The gold pads and electrodes were fabricated on top of the nanowires using the photolithographic procedure detailed in Chapter 2. Figure 5.1 shows a sample of the nanowires trapped under gold electrodes, prepared for a 4-point-probe measurement, immediately after deposition and lift-off. Samples of the 20 μm pad pattern were also created with silver nanowires bridging between two pads. The choice of 20 μm for spacing is appropriate since the nanowires average about 40 μm and the next step of pad distance available on the mask was 60 μm.

5.2 Resistivity measurements

Resistivity measurements were performed using the 4-point-probe apparatus with nanowires trapped underneath gold electrodes attached to probeable gold pads. Figure 5.1 shows an example of this formation. The principles of 4-point-probe measurement are explained in Chapter 1 and the structure and method of deposition of the gold electrodes are explained in Chapter 2.

Figure 5.2 shows an example of a nanowire probed using the 4-point-probe measurement with the results shown to the right. Using the two middle voltage probes, the resistance

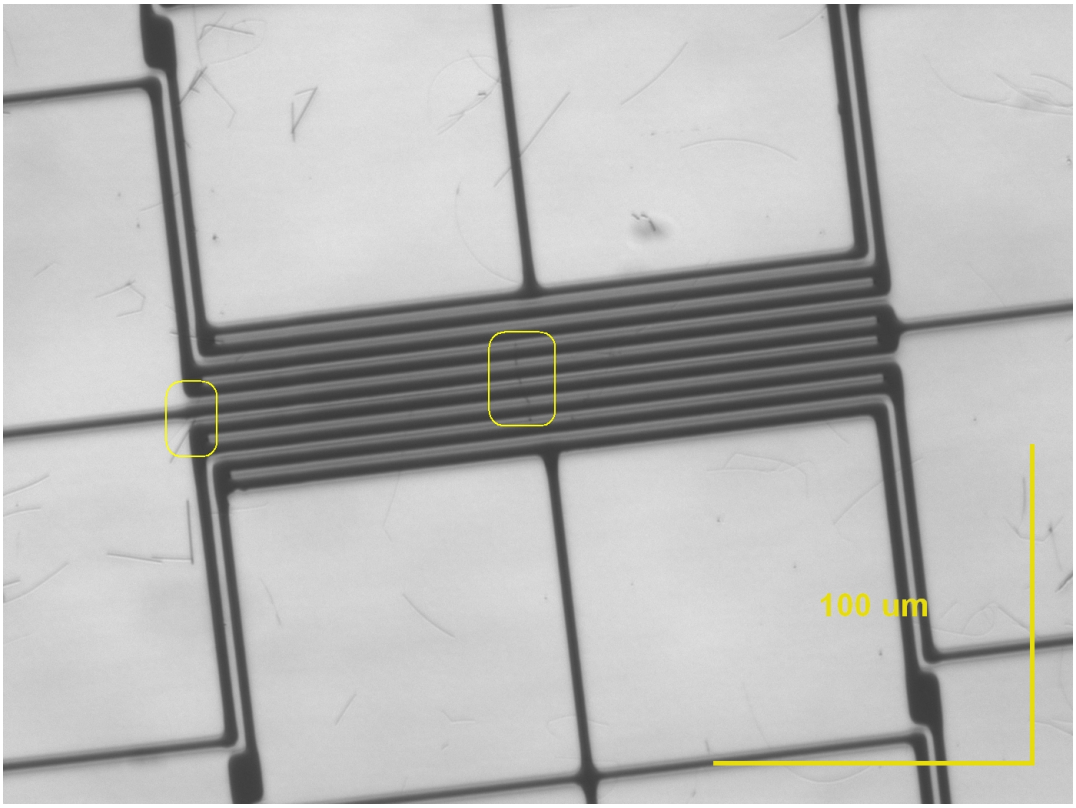

Figure 5.1: Nanowire-electrode devices, immediately after deposition and lift off, taken using an optical microscope.

of the nanowire in this case was measured to be 41 Ω with the resistivity coming to 2.0x10^{-7}Ω·m.

Overall three nanowires were tested that had resistivities between 2.0x10^{-7} Ω·m to 4.8x10^{-7} Ω·m. This is only slightly above measured nanowire resistivities in literature, which generally comes within the 3.0x10^{-8} Ω·m to 1.5x10^{-7} Ω·m range [25, 32, 70, 73, 80]. The slightly larger resistance could be attributed to the pentagonally twinned structure of the nanowires and the fact that the nanowires are not circularly shaped, both of which lead to larger electron scattering. The resistivity of bulk silver is 1.6x10^{-8} Ω·m.

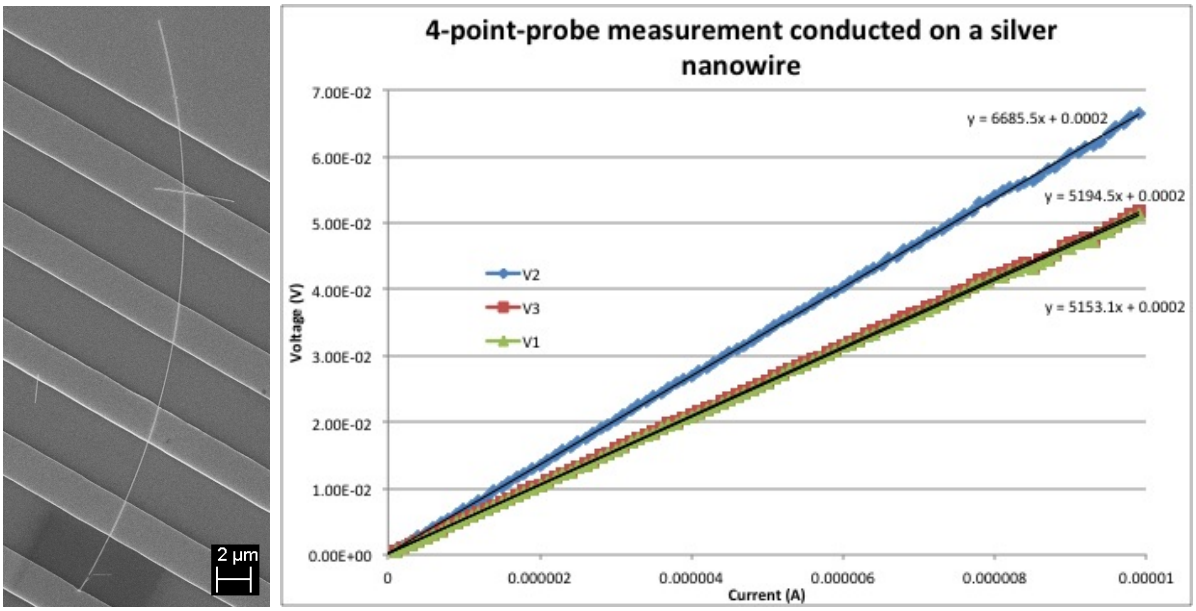

Figure 5.2: A 4-point-probe resistivity measurement (right) is conducted on a silver nanowire connected to gold electrodes (left). The resistivity of this nanowires comes to $2.0\text{x}10^{-7}\Omega\cdot\text{m}$

5.3 Welding results

A 2-point-probe connection was patterned to weld the same nanowires to the deposited gold pads. Nanowires that were situated between two gold pads were located using the optical microscope and were probed using a probe station and a common semiconductor analyzer. An example of this nanowire-pad construction is illustrated in Figure 5.3.

These nanowires, like the nanowires in Chapter 4, initially displayed a diode-like response. The order of voltage and current sweeps used to weld the nanowires to the pads is explained in Chapter 4 Section 4.3.1. Figure 5.4 is a collection of select voltage and current responses to current and voltage sweeps respectively.

Figure 5.4a shows a very similar response to the one observed when welding two similar nanowires together in Chapter 4. Once the "surge" voltage reaches a level that is feasible for a current stimulus, current sweep measurements begin. Although just a representative of many measurements of this type conducted, Sweep #1 in Figure 5.4b shows the process by which current can weld the nanowire. Each one of the drops in the voltage response in Sweep #1 represent a point of welding. The nanowire first becomes ohmic, and then

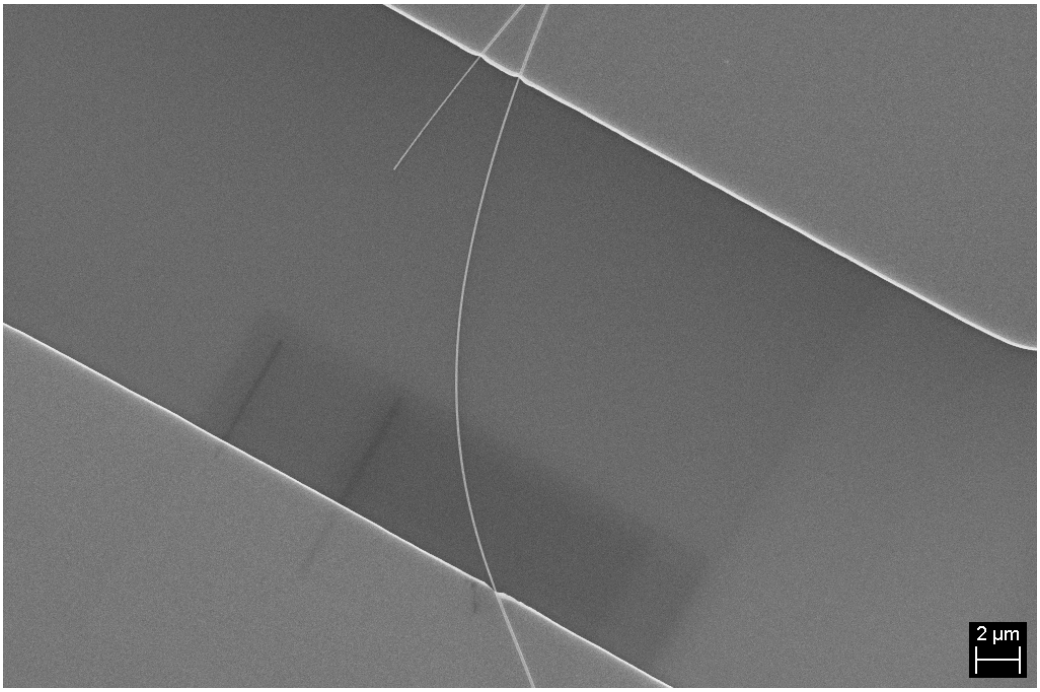

Figure 5.3: A nanowire is trapped between two gold pads ready for the welding procedure

remains ohmic with a lower resistance. After several current sweeps with increasing sweep maximums, a current level will be reached where the nanowire is permanently ohmic with a very low resistance. Experience driving nanowires into failure was the only guide for when to stop the welding. The I-V response of the nanowire after the welding process is represented by Sweep #2 in Figure 5.4b. The resistance of the nanowire at this point is measured to be 273 Ω and the resistivity is measured to be $4.5\text{x}10^{-7}$ Ω·m. This value is only twice the lowest measured resistivity using the 4-point-probe technique. This weld was constant and reliable for a period of time on the order of days.

Three other nanowires were welded to gold pads and had calculated resistivities of $1.4\text{x}10^{-6}$ Ω·m, $3.5\text{x}10^{-7}$ Ω·m, and $2.3\text{x}10^{-7}$ Ω·m.

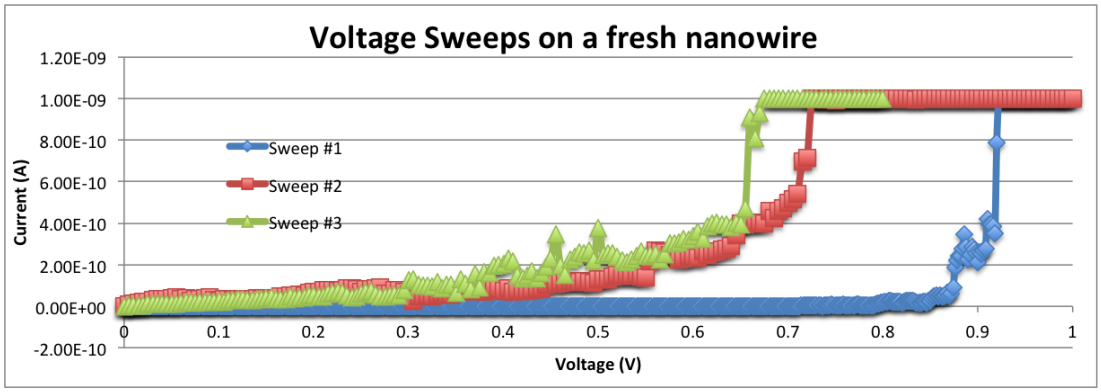

(a)

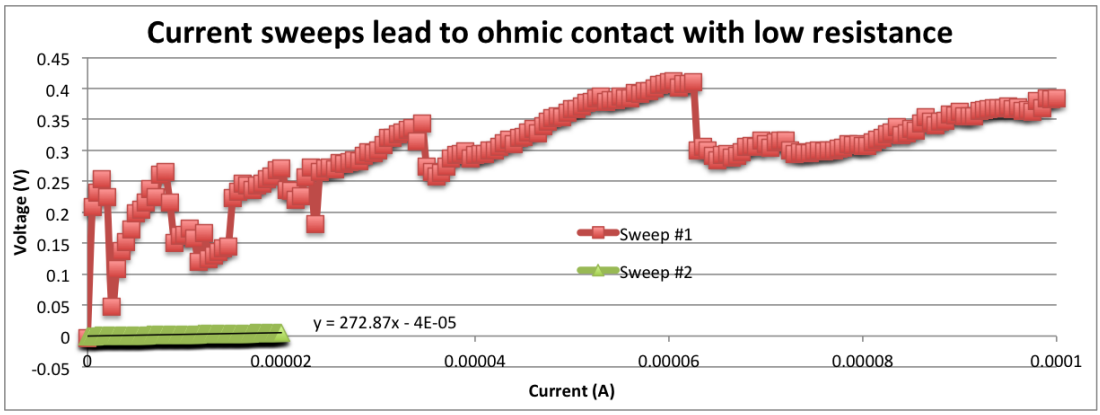

(b)

Figure 5.4: (a) The current response to a selection of voltage sweeps are shown. The maximum current is set at 1 nA for all measurements. (b) The voltage responses to selected current sweeps are shown. Sweep #2 is the final ohmic result.

5.4 Analysis

5.4.1 Reduction in contact resistance

To analyze the changes in contact resistance, one must measure the resistance (which inherently includes the contact resistance) before welding begins, and compare the final welded resistance to the one measured using the 4-point-probe technique. One can calculate the initial resistance using the first voltage sweep measurement conducted on each nanowire, with voltage running up to 0.5 V. For the same nanowire, that has the data displayed in

Figure 5.4, a resistance of 1.1x10^{14} Ω is measured at the outset. An equation is proposed for calculating the percent reduction in contact resistance as follows:

$$r = \frac{R_i - R_f}{R_i - R_n} \times 100\% \tag{5.1}$$

where R_i is the initial resistance, R_f is the final resistance, and R_n is the resistance of the nanowire calculated by using the dimensions and a resistivity of 2x10^{-7} Ω·m, the lowest measured using 4 probes ($R = \rho\frac{l}{A}$). In Equation 5.1 the numerator of the fraction represents the actual reduction in contact resistance, while the denominator represents the total contact resistance calculated using expected resistivity. Using the values above, one calculates a reduction in resistance of nearly 100% for that particular nanowire (see #4 in the table in Figure 5.5). Figure 5.5 shows a table created to demonstrate the results of welding nanowires to their contacts. Almost all the nanowires that had the welding applied to them had a reduction in contact resistance of nearly 100%.

Nanowire	Initial resistance Ω	Final resistance Ω	Nanowire resistance Ω	% reduction
#1	3.3E+12	355	299	99.9999999983
#2	2.5E+12	273	157	99.9999999953
#3	1.1E+12	1529	225	99.9999998815
#4	1.1E+14	273	115	99.9999999999

Figure 5.5: A table collecting data from the nanowires that had the welding procedure applied to them. The final column is a calculation of the percentage drop in contact resistance contribution to overall resistivity. This value is calculated using Equation 5.1

The table shown in Figure 5.5 is an important testament to the repeatability and the reliability of our method of reducing contact resistance. The near-complete abolition of contact resistance has not yet been reported to the best of my knowledge.

5.4.2 Reliability

To test out the reliability of the nanowires, once the weld was complete, the nanowires were tested for resistance values in subsequent time intervals. All the nanowires were permanent in the final welding form for at least 2 hours. Nanowires #3 and #4 were tested 6 days after the final weld procedure was complete, and both exhibited ohmic characteristics. Nanowire #3 had an increase in resistance of ∼2000% and nanowire #4 had an increase in resistance of ∼40% after 6 days. The other nanowires were no longer fully ohmic after 6 days,

although they quickly became ohmic upon a second measurement. The voltage response of the latter nanowires was also much smaller than what it was before any welding was done, meaning the nanowires had not completely reverted to the pre-weld status.

There can be several reasons for why the nanowire welds disintegrate over time. Khaligh and Goldthorpe [77] showed that the corrosion of polyol synthesized silver nanowires speeds up with applied heat. Since the welding currents have gone as high as 3mA, the heating done on the nanowires could have caused a spike in corrosion, which could then reintroduce an intermediate layer, or simply increase resistivity through surface contaminants. Another reason could be that the welding procedure causes the alloying of the gold and the silver, which due to high surface mobility of silver could cause cracks in the nanowires [70]. A small disconnect would raise resistance significantly. A further possibility is that the weld does not completely join the silver and the gold but rather welds in pieces close to the edge of the contact. With the nature of the silver-gold junction changing along the nanowire surface under the pad, a stress can be exerted that eventually drives the gold and the silver apart again.

5.4.3 Failure

The image shown in Figure 5.2 is of a nanowire that has already gone through the welding process. Indeed most of the nanowires taken through the process, including the four investigated in Section 5.4.1, survived the procedure. A few nanowires however did not. Figure 5.6 shows the only two examples of such nanowires out of 12 nanowires investigated.

The burning pattern as expected follows Tohmyoh's predictions [18]. All the burning around the nanowire are either at the contacts, where a majority of the heat is produced, or in the center of two contacts on the nanowire.

5.5 Limitations

The main limitation of our investigation of lowering contact resistance is the use of separate nanowires for the tests. It has been previously discovered that nanowire resistivity changes with diameter, and the nanowires used for 4-point-probe measurements do not necessarily have the same resistivity as the nanowires used in the welding process. Although this makes the measurements slightly inaccurate, the inaccuracy is negligible as compared to the reduction in contact resistance, and the main result of our study remains valid.

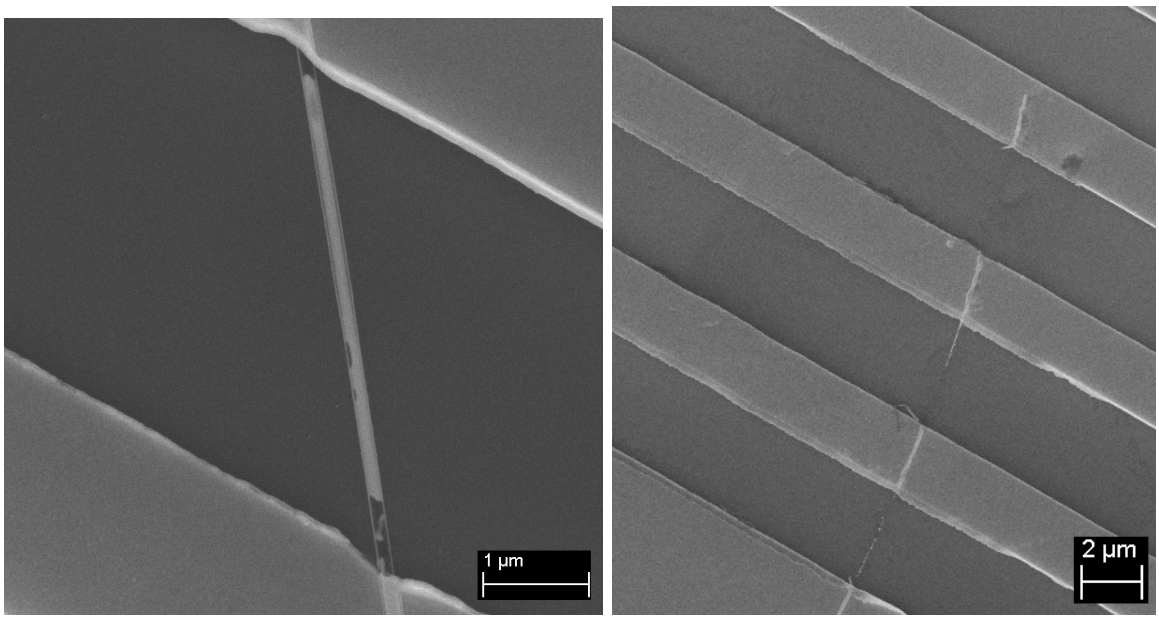

Figure 5.6: Nanowires burnt in the welding process

Chapter 6

Conclusion and future work

6.1 Conclusion

In this thesis a simple and economical process for electrically accessing nanostructures was designed and implemented, and it was used to characterize and weld silver nanowires. The process was a combination of dispersion drop-casting and photolithography with efficient mask design. The procedure was faster, simpler, and the machinery more readily available than methods used to create contact nanowires by others in the literature. Furthermore, the welding of easily synthesized polyol silver nanowires has never been done before. Although contact resistance reduction had been attempted using Joule-heat welding, no such project had yet been able to nearly completely reduce contact resistance between electrodes and metal nanowires.

A novel form of nanobeams created using diffusion bonding in solution was then characterized using the method designed. This type of nanobeam was created by joining together silver nanoplates synthesized using the polyol process. By characterizing these nanobeams it was confirmed that the electrical response matched that of a crystalline nanostructure. This corroborates with previous computer models that have predicted the nanodisks will realign while joining to line up the crystal lattice structure.

Polyol nanowires were then put in series between two gold pads fabricated using the photolithographic process. Electrical voltage or current was then forced through the two nanowires in a specific order, initiating a reliable weld. The advantages of Joule-heating compared to other forms of welding was discussed. Joule-heating is found to be simple to execute, inexpensive to set up, and quick. Furthermore, the apparatus required for Joule-heating is much more likely to be mountable on an assembly line. Using Joule heating silver

nanowire overlapped and gap junctions were welded together in an ohmic low resistance connection. The mechanism by which gap junctions fill the void was also investigated and it was found that heat generated melts the wire closest to the junction, allowing it to fill the gap.

The initial rectifying characteristics of nanowire contacts were also investigated. It was found that the response largely mirrors that of a Schottky diode and that is likely due to the presence of an intermediate layer between the two nanowires or the nanowire-pad junction. A procedure is created to break down this Schottky contact and establish an ohmic connection without major damage to the nanowires. This can be paramount to the metal contact fabrication facilities, for they go through many extra steps and demand expensive equipment to avoid the Schottky type contacts. Potentially large amounts of expense can be avoided by simply applying our electrical regiment to loosely fabricated contacts.

Lastly, commercially available polyol silver nanowires were welded to gold pads to reduce contact resistance for accurate 2-point-probe measurements. It was found that the nanowire gold pad apparatus also has a Schottky response, and with the aid of the electrical recipe used to weld nanowires, the contact was made ohmic, with the overall system 2-point-probe resistivity being as low as $2.3\text{x}10^{-7}$ Ω·m. A survey of four nanowires showed that in almost all cases the contribution from contact resistance to resistivity was reduced by nearly 100% compared to resistivities measured using 4-point-probe measurements.

6.2 Future work

- A further investigation into the causes of weld separation seems like the logical place to start. No other papers to my knowledge have yet to explore the long-term reliability of their welds, most likely due to observing the same pattern. A time-step based TEM analysis of the weld region with a side-by-side time-step electrical characterization would likely shed much light onto the causes of long term weld failure.

- Another point of future focus could be the control system integration of the electrical recipe created for breaking down Schottky contacts and establishing ohmic connections. The possibility of mounting such a device on an assembly line would find industrial applications if attempted.

- Finally, an extension of the nanowire-electrode welding procedure would find great uses. To be able to show that this method can reduce contact resistance in the

electrode junctions of a variety of metallic wires, and possibly semiconducting wires, would make experimentation on such wires much easier in times ahead.

References

[1] J. Salfi, U. Philipose, C. F. De Sousa, S. Aouba, and H.E. Ruda. Electrical properties of ohmic contacts to znse nanowires and their application to nanowire-based photodetection. *Applied Physics Letters*, 89(26):261112–261112–3, 2006.

[2] Colby A. Foss, Gabor L. Hornyak, Jon A. Stockert, and Charles R. Martin. Optically transparent nanometal composite membranes. *Advanced Materials*, 5(2):135–136, 1993.

[3] X. Duan, Y. Huang, Y. Cui, J. Wang, and C. M. Lieber. Indium phosphide nanowires as building blocks for nanoscale electronic and optoelectronic devices. *Nature*, 409:66–69, 2001.

[4] Zhi-Min Liao, Jia-Bin Xu, Xiao-Ming Sun, Ya-Dong Li, Jun Xu, and Da-Peng Yu. Quantum interference effect in single disordered silver nanowires. *Physics Letters A*, 373(1213):1181 – 1184, 2009.

[5] Haiqing Liu, Jun Kameoka, David A. Czaplewski, and H. G. Craighead. Polymeric nanowire chemical sensor. *Nano Letters*, 4(4):671–675, 2004.

[6] Erik C. Garnett, Mark L. Brongersma, Yi Cui, and Michael D. McGehee. Nanowire solar cells. *Annual Review of Materials Research*, 41(1):269–295, 2011.

[7] Junya Suehiro, Nobutaka Nakagawa, Shin ichiro Hidaka, Makoto Ueda, Kiminobu Imasaka, Mitsuhiro Higashihata, Tatsuo Okada, and Masanori Hara. Dielectrophoretic fabrication and characterization of a zno nanowire-based uv photosensor. *Nanotechnology*, 17(10):2567, 2006.

[8] Benjamin J. Wiley, Sang Hyuk Im, Zhi-Yuan Li, Joeseph McLellan, Andrew Siekkinen, and Younan Xia. Maneuvering the surface plasmon resonance of silver nanostructures through shape-controlled synthesis. *The Journal of Physical Chemistry B*, 110(32):15666–15675, 2006.

[9] Jong-in Hahm and Charles M. Lieber. Direct ultrasensitive electrical detection of dna and dna sequence variations using nanowire nanosensors. *Nano Letters*, 4(1):51–54, 2004.

[10] Robin S. Friedman, Michael C. McAlpine, David S. Ricketts, Donhee Ham, and Charles M. Lieber. Nanotechnology: High-speed integrated nanowire circuits. *Nature*, (7037):10851085, 2005.

[11] Anna L. Pyayt, Benjamin Wiley, Younan Xia, Antao Chen, and Larry Dalton. Integration of photonic and silver nanowire plasmonic waveguides. *Nat Nano*, 3(11):660–665, November 2008.

[12] Catalina Marambio-Jones and EricM.V. Hoek. A review of the antibacterial effects of silver nanomaterials and potential implications for human health and the environment. *Journal of Nanoparticle Research*, 12(5):1531–1551, 2010.

[13] Andrea Tao, Franklin Kim, Christian Hess, Joshua Goldberger, Rongrui He, Yugang Sun, Younan Xia, and Peidong Yang. Langmuirblodgett silver nanowire monolayers for molecular sensing using surface-enhanced raman spectroscopy. *Nano Letters*, 3(9):1229–1233, 2003.

[14] F. Fievet, J. P. Lagier, and M. Figlarz. Preparing monodisperse metal powders in micrometer and submicrometer sizes by the polyol process. *MRS Bull*, 14:29–34, 1989.

[15] Peng Peng, Anming Hu, Hong Huang, Adrian P. Gerlich, Boxin Zhao, and Y. Norman Zhou. Room-temperature pressureless bonding with silver nanowire paste: towards organic electronic and heat-sensitive functional devices packaging. *J. Mater. Chem.*, 22:12997–13001, 2012.

[16] Y. Sun and Y. Xia. Large-scale synthesis of uniform silver nanowires through a soft, self-seeding, polyol process. *Advanced Materials*, 14(11):833–837, 2002.

[17] Benjamin Wiley, Yugang Sun, and Younan Xia. Synthesis of silver nanostructures with controlled shapes and properties. *Accounts of Chemical Research*, 40(10):1067–1076, 2007.

[18] Hironori Tohmyoh. A governing parameter for the melting phenomenon at nanocontacts by joule heating and its application to joining together two thin metallic wires. *Journal of Applied Physics*, 105(1):014907, 2009.

[19] Hironori Tohmyoh and Masato Fujimori. Microstructural and electrical characterization of joule heat welds in ultrathin pt wires. *Physica E: Low-dimensional Systems and Nanostructures*, 46(0):33 – 37, 2012.

[20] Ehsan Marzbanrad, Anming Hu, Boxin Zhao, and Y. N. Zhou. Room temperature nanojoining of triangular and hexagonal silver nanodisks. Submitted, 2013.

[21] Damian Aherne, Deirdre M. Ledwith, Matthew Gara, and John M. Kelly. Optical properties and growth aspects of silver nanoprisms produced by a highly reproducible and rapid synthesis at room temperature. *Advanced Functional Materials*, 18(14):2005–2016, 2008.

[22] Baruch Feldman, Seongjun Park, Michael Haverty, Sadasivan Shankar, and Scott T. Dunham. Simulation of grain boundary effects on electronic transport in metals, and detailed causes of scattering. *physica status solidi (b)*, 247(7):1791–1796, 2010.

[23] L. K J Vandamme. Noise as a diagnostic tool for quality and reliability of electronic devices. *Electron Devices, IEEE Transactions on*, 41(11):2176–2187, 1994.

[24] S.A. Campbell. *The Science and Engineering of Microelectronic Fabrication*. The Oxford Series in Electrical and Computer Engineering. Oxford University Press, 2001.

[25] Qiaojian Huang, C.M. Lilley, and M. Bode. Surface scattering effect on the electrical resistivity of single crystalline silver nanowires self-assembled on vicinal si (001). *Applied Physics Letters*, 95(10):103112–103112–3, 2009.

[26] A A Talin, F Leonard, A M Katzenmeyer, B S Swartzentruber, S T Picraux, M E Toimil-Molares, J G Cederberg, X Wang, S D Hersee, and A Rishinaramangalum. Transport characterization in nanowires using an electrical nanoprobe. *Semiconductor Science and Technology*, 25(2):024015, 2010.

[27] R Lin, M Bammerlin, O Hansen, R R Schlittler, and P Bøggild. Micro-four-point-probe characterization of nanowires fabricated using the nanostencil technique. *Nanotechnology*, 15(9):1363, 2004.

[28] Josh Goldberger, Donald J. Sirbuly, Matt Law, and Peidong Yang. Zno nanowire transistors. *The Journal of Physical Chemistry B*, 109(1):9–14, 2005.

[29] Steve Reyntjens and Robert Puers. A review of focused ion beam applications in microsystem technology. *Journal of Micromechanics and Microengineering*, 11(4):287, 2001.

[30] Willem F. van Dorp, Bob van Someren, Cornelis W. Hagen, Pieter Kruit, and Peter A. Crozier. Approaching the resolution limit of nanometer-scale electron beam-induced deposition. *Nano Letters*, 5(7):1303–1307, 2005.

[31] L. Liao, H. B. Lu, J. C. Li, C. Liu, D. J. Fu, and Y. L. Liu. The sensitivity of gas sensor based on single zno nanowire modulated by helium ion radiation. *Applied Physics Letters*, 91(17):173110, 2007.

[32] Wenhua Gu, Hyungsoo Choi, and Kyekyoon (Kevin) Kim. Universal approach to accurate resistivity measurement for a single nanowire: Theory and application. *Applied Physics Letters*, 89(25):253102, 2006.

[33] E Schlenker, A Bakin, T Weimann, P Hinze, D H Weber, A Gölzhäuser, H-H Wehmann, and A Waag. On the difficulties in characterizing zno nanowires. *Nanotechnology*, 19(36):365707, 2008.

[34] T Hanrath and B. A. Korgel. Germanium nanowire transistors: A comparison of electrical contacts patterned by electron beam lithography and beam-assisted chemical vapour deposition. *Proceedings of the Institution of Mechanical Engineers, Part N: Journal of Nanoengineering and Nanosystems*, 218(1):25–34, 2004.

[35] Vidyut Gopal, Velimir R. Radmilovic, Chiara Daraio, Sungho Jin, Peidong Yang, and Eric A. Stach. Rapid prototyping of site-specific nanocontacts by electron and ion beam assisted direct-write nanolithography. *Nano Letters*, 4(11):2059–2063, 2004.

[36] A. Vilá, F. Hernàndez-Ramirez, J. Rodrìguez, O. Casals, A. Romano-Rodìguez, J.R. Morante, and M. Abid. Fabrication of metallic contacts to nanometre-sized materials using a focused ion beam (fib). *Materials Science and Engineering: C*, 26(57):1063 – 1066, 2006. ¡ce:title¿Current Trends in Nanoscience - from Materials to Applications¡/ce:title¿ ¡xocs:full-name¿Proceedings of the European Materials Research Society 2005 - Symposium A¡/xocs:full-name¿.

[37] M. E. Toimil Molares, E. M. Höhberger, Ch. Schaeflein, R. H. Blick, R. Neumann, and C. Trautmann. Electrical characterization of electrochemically grown single copper nanowires. *Applied Physics Letters*, 82(13):2139–2141, 2003.

[38] E Stern, G Cheng, E Cimpoiasu, R Klie, S Guthrie, J Klemic, I Kretzschmar, E Steinlauf, D Turner-Evans, E Broomfield, J Hyland, R Koudelka, T Boone, M Young, A Sanders, R Munden, T Lee, D Routenberg, and M A Reed. Electrical characterization of single gan nanowires. *Nanotechnology*, 16(12):2941, 2005.

[39] Sang Won Yoon, Jong Hyun Seo, Kyou-Hyun Kim, Jae-Pyoung Ahn, Tae-Yeon Seong, Kon Bae Lee, and Hoon Kwon. Electrical properties and microstructural characterization of single zno nanowire sensor manufactured by {FIB}. *Thin Solid Films*, 517(14):4003 – 4006, 2009. The proceedings of the 1st International Conference on Microelectronics and Plasma Technology (ICMAP 2008).

[40] P Parkinson, N Jiang, Q Gao, H H Tan, and C Jagadish. Direct-write nonlinear photolithography for semiconductor nanowire characterization. *Nanotechnology*, 23(33):335704, 2012.

[41] David J. Griffiths. *Introduction to Electrodynamics (3rd Edition)*. Benjamin Cummings, 1998.

[42] H. G. Craighead. Nanoelectromechanical systems. *Science*, 290(5496):1532–1535, 2000.

[43] Gregory S Snider and R Stanley Williams. Nano/cmos architectures using a field-programmable nanowire interconnect. *Nanotechnology*, 18(3):035204, 2007.

[44] Harald Ditlbacher, Andreas Hohenau, Dieter Wagner, Uwe Kreibig, Michael Rogers, Ferdinand Hofer, Franz R. Aussenegg, and Joachim R. Krenn. Silver nanowires as surface plasmon resonators. *Phys. Rev. Lett.*, 95:257403, Dec 2005.

[45] Mingwei Li, Rustom B. Bhiladvala, Thomas J. Morrow, James A. Sioss, Kok-Keong Lew, Joan M. Redwing, Christine D. Keating, and Theresa S. Mayer. Bottom-up assembly of large-area nanowire resonator arrays. *Nat Nano*, 3:88–92, 2008.

[46] Yue Wu, Jie Xiang, Chen Yang, Wei Lu, and Charles M. Lieber. Single-crystal metallic nanowires and metal/semiconductor nanowire heterostructures. *Nature*, (6995):6165, 2004.

[47] Mei Li, Heimo Schnablegger, and Stephen Mann. Coupled synthesis and self-assembly of nanoparticles to give structures with controlled organization. *Nature*, 402(6760):393–395, Nov 25 1999.

[48] Zhiyong Tang, Nicholas A. Kotov, and Michael Giersig. Spontaneous organization of single cdte nanoparticles into luminescent nanowires. *Science*, 297(5579):237–240, 2002.

[49] Catherine J. Murphy, Tapan K. Sau, Anand M. Gole, Christopher J. Orendorff, Jinxin Gao, Linfeng Gou, Simona E. Hunyadi, and Tan Li. Anisotropic metal nanoparticles:

synthesis, assembly, and optical applications. *The Journal of Physical Chemistry B*, 109(29):13857–13870, 2005. PMID: 16852739.

[50] Changxin Chen, Lijun Yan, Eric Siu-Wai Kong, and Yafei Zhang. Ultrasonic nanowelding of carbon nanotubes to metal electrodes. *Nanotechnology*, 17(9):2192, 2006.

[51] Yang Lu, Jian Yu Huang, Chao Wang, Shouheng Sun, and Jun Lou. Cold welding of ultrathin gold nanowires. *Nature Nanotechnology*, 5(3):218224, 2010.

[52] Peng Peng, Lei Liu, Adrian P. Gerlich, Anming Hu, and Y. Norman Zhou. Self-oriented nanojoining of silver nanowires via surface selective activation. *Particle & Particle Systems Characterization*, 30(5):420–426, 2013.

[53] Yong Peng, Tony Cullis, and Beverley Inkson. Bottom-up nanoconstruction by the welding of individual metallic nanoobjects using nanoscale solder. *Nano Letters*, 9(1):91–96, 2009.

[54] Çağlar Ö. Girit and A. Zettl. Soldering to a single atomic layer. *Applied Physics Letters*, 91(19):193512, 2007.

[55] Zhiyong Gu, Hongke Ye, Diana Smirnova, David Small, and DavidH. Gracias. Reflow and electrical characteristics of nanoscale solder. *Small*, 2(2):225–229, 2006.

[56] D von der Linde, K Sokolowski-Tinten, and J Bialkowski. Lasersolid interaction in the femtosecond time regime. *Applied Surface Science*, 109110(0):1 – 10, 1997.

[57] Seol Ji Kim and Du-Jeon Jang. Laser-induced nanowelding of gold nanoparticles. *Applied Physics Letters*, 86(3):033112, 2005.

[58] Xiaojie Duan, Jin Zhang, Xing Ling, and Zhongfan Liu. Nano-welding by scanning probe microscope. *Journal of the American Chemical Society*, 127(23):8268–8269, 2005.

[59] Shengyong Xu, Mingliang Tian, Jinguo Wang, Jian Xu, Joan Redwing, and Moses Chan. Nanometer-scale modification and welding of silicon and metallic nanowires with a high-intensity electron beam. *Small*, 1(12):1221–1229, 2005.

[60] Zhenxia Wang, Liping Yu, Wei Zhang, Yinfeng Ding, Yulan Li, Jiaguang Han, Zhiyuan Zhu, Hongjie Xu, Guowei He, Yi Chen, and Gang Hu. Amorphous molecular junctions produced by ion irradiation on carbon nanotubes. *Physics Letters A*, 324(4):321 – 325, 2004.

[61] Robert N. Barnett, Hannu Häkkinen, Andrew G. Scherbakov, and Uzi Landman. Hydrogen welding and hydrogen switches in a monatomic gold nanowire. *Nano Letters*, 4(10):1845–1852, 2004.

[62] Khim Karki, Eric Epstein, Jeong-Hyun Cho, Zheng Jia, Teng Li, S. Tom Picraux, Chunsheng Wang, and John Cumings. Lithium-assisted electrochemical welding in silicon nanowire battery electrodes. *Nano Letters*, 12(3):1392–1397, 2012.

[63] EC Garnett, W Cai, JJ Cha, F Mahmood, ST Connor, M Greyson Christoforo, Y Cui, MD McGehee, and ML Brongersma. Self-limited plasmonic welding of silver nanowire junctions. *Nature materials*, 11(3):241–249, 03 2012.

[64] JoshuaA. Spechler and CraigB. Arnold. Direct-write pulsed laser processed silver nanowire networks for transparent conducting electrodes. *Applied Physics A*, 108(1):25–28, 2012.

[65] H. Hirayama, Y. Kawamoto, Y. Ohshima, and K. Takayanagi. Nanospot welding of carbon nanotubes. *Applied Physics Letters*, 79(8):1169–1171, 2001.

[66] Lifeng Dong, Steven Youkey, Jocelyn Bush, Jun Jiao, Valery M. Dubin, and Ramanan V. Chebiam. Effects of local joule heating on the reduction of contact resistance between carbon nanotubes and metal electrodes. *Journal of Applied Physics*, 101(2):024320, 2007.

[67] Tan Yu and Wang Yan-Guo. Elimination of the schottky barrier at an au-znse nanowire nanocontact via in situ joule heating. *Chinese Physics Letters*, 30(1):017902, 2013.

[68] Tan Yu and Wang Yan-Guo. Current density-sensitive welding of a semiconductor nanowire to a metal electrode. *Chinese Physics Letters*, 30(1):017901, 2013.

[69] J. Muster, G. T. Kim, V. Krsti, J. G. Park, Y. W. Park, S. Roth, and M. Burghard. Electrical transport through individual vanadium pentoxide nanowires. *Advanced Materials*, 12(6):420–424, 2000.

[70] Benjamin J. Wiley, Zenghui Wang, Jiang Wei, Yadong Yin, David H. Cobden, and Younan Xia. Synthesis and electrical characterization of silver nanobeams. *Nano Letters*, 6(10):2273–2278, 2006.

[71] Takehiro Tokuno, Masaya Nogi, Makoto Karakawa, Jinting Jiu, ThiThi Nge, Yoshio Aso, and Katsuaki Suganuma. Fabrication of silver nanowire transparent electrodes at room temperature. *Nano Research*, 4(12):1215–1222, 2011.

[72] B. Hammer and J. K. Norskov. Why gold is the noblest of all the metals. *Nature*, 376(6537):238–240, 1995.

[73] Stela Pruneanu, Liliana Olenic, Said A. Farha Al-Said, Gheorghe Borodi, Andrew Houlton, and BenjaminR. Horrocks. Template and template-free preparation of one-dimensional metallic nanostructures. *Journal of Materials Science*, 45(12):3151–3159, 2010.

[74] Aveek Bid, Achyut Bora, and A. K. Raychaudhuri. Temperature dependence of the resistance of metallic nanowires of diameter $\geqslant$ 15 nm: Applicability of bloch-grüneisen theorem. *Phys. Rev. B*, 74:035426, Jul 2006.

[75] Jose Luis Elechiguerra, Leticia Larios-Lopez, Cui Liu, Domingo Garcia-Gutierrez, Alejandra Camacho-Bragado, and Miguel Jose Yacaman. Corrosion at the nanoscale: the case of silver nanowires and nanoparticles. *Chemistry of Materials*, 17(24):6042–6052, 2005.

[76] M. Radmilović-Radjenović and B. Radjenović. An analytical relation describing the dramatic reduction of the breakdown voltage for the microgap devices. *EPL (Europhysics Letters)*, 83(2):25001, 2008.

[77] Hadi Hosseinzadeh Khaligh and Irene A. Goldthorpe. Failure of silver nanowire transparent electrodes under current flow. *Nanoscale Research Letters*, 8(1):1–6, 2013.

[78] Aveek Bid, Achyut Bora, and A. K. Raychaudhuri. Observation of large low-frequency resistance fluctuations in metallic nanowires: Implications on its stability. *Phys. Rev. B*, 72:113415, Sep 2005.

[79] A. Graff, D. Wagner, H. Ditlbacher, and U. Kreibig. Silver nanowires. *The European Physical Journal D - Atomic, Molecular, Optical and Plasma Physics*, 34(1-3):263–269, 2005.

[80] Sung Ha Park, Matthew W. Prior, Thomas H. LaBean, and Gleb Finkelstein. Optimized fabrication and electrical analysis of silver nanowires templated on dna molecules. *Applied Physics Letters*, 89(3):033901–033901–3, 2006.